Superfluidity and the magnetic field of pulsars

D. M. Sedrakyan and K. M. Shakhabasyan

Byurakan Astrophysical Observatory, Erevan State University

(Submitted 10 October, 1990; resubmitted after revision 21 January, 1991)
Usp. Fiz. Nauk, **161**, 3–40 (July 1991)

The current state of the theory of superfluidity in pulsars is presented. The superfluidity of hadronic matter in neutron stars is considered. It is shown that strong interaction between the neutron and proton condensates leads to a drag current of superconducting protons and to the generation of a strong time-independent magnetic field ($B = 10^{12}$ G) parallel to the axis of rotation. The strength of this field depends on the microscopic parameters of the superfluid hadrons. Models explaining the origin of glitches and postglitch relaxation are discussed. The coupling time between the neutron superfluid and the rigid crust of the neutron star is calculated.

Pulsars are objects that emit stable periodic radio pulses and are among the most remarkable entities in our Galaxy.[1,2] They are effectively unique cosmic laboratories that provide a testing ground for the interplay, application, and verification of many ideas drawn from different branches of physics, e.g., gravitation, nuclear physics, low-temperature physics, and plasma physics. There are many important unanswered questions despite the substantial advances in our understanding of the physical processes in pulsars since the discovery[3] of pulsars in 1967 and their identification[4] as rotating neutron stars. It is now firmly established that pulsars are rapidly rotating neutron stars with a very strong magnetic field.[5] The radiation emitted by pulsars is highly polarized (45–95% in the case of the pulsar PSR 0833), which indicates that the radiating regions lie in a very strong magnetic field. The strength of this field has been estimated from experimental data on x-ray pulsars in binary systems. In 1976, balloon observations[6,7] of the spectrum of pulsar HER-X-1 revealed the presence of a very narrow emission at 58 ± 5 keV with intensity $I = 3\times 10^{-3}$ photons/cm^2 s, which was due to cyclotron emission[8,9] by electrons traveling in a magnetic field $H \approx 5\times 10^{12}$ Oe. In 1977, the presence of the narrow line $E_\gamma \approx 64$ keV in the hard x-ray emission of pulsar HER X-1 (period 1.24 s) was confirmed by observations from the Ariel 5 satellite.[10] The cyclotron line at $E_\gamma \approx 11$–20 keV has also been observed[11] in the spectrum of the x-ray pulsar 4U0115 + 63. The magnetic field of this pulsar was reported[12] as being of the order of 1.2×10^{12} Oe.

A similar feature has also been seen at $E_\gamma \approx 80$ keV in the x-ray spectrum of the Crab nebula. Its intensity was found to vary with a period of 33 ms, i.e., the rotational period of pulsar PSR 0531 + 21 in the Crab nebula.[13,14] Observational data are thus seen to suggest the presence of a strong magnetic field in pulsars.

Another remarkable property of pulsars is the superfluidity of their interior, which has a significant influence on the dynamics of their rotation.

The very earliest observations[15] demonstrated the surprising stability of the basic pulsation periods. They can be predicted, in some cases, to better than 10^{-12} over an interval of several years, i.e., almost with the precision of atomic frequency standards. It has therefore been suggested that millisecond pulsars, with the highest stability of emission periodicity, could serve as highly accurate providers of an astronomic time scale.

The frequency derivative $\dot{\Omega}$ of pulsars for which there is an adequate supply of observational data is always negative, i.e., the period p increases with time. This monotonic increase in the period is called the secular variation and is due to the loss of rotational energy and of angular momentum by the neutron star.[16–18] This secular variation was first discovered for the Crab pulsar[19] for which $\dot{p} = 4.2\times 10^{-13}$ s/s. The highest value of the derivative, i.e., $\dot{p} = 1.54\times 10^{-12}$ s/s, was recorded for pulsar PSR 1508-59 which has $p = 150$ ms [20] and lies in the remnant of the shell-type supernova MSH 15-52. The smallest derivative among those measured so far, i.e., $\dot{p} = 3.2\times 10^{-20}$ s/s, has been reported for the millisecond pulsar PSR 1953 + 29 which has $p = 6.1$ ms and is part of a binary system. We note that the shortest known period $p = 1.557$ ms, is that of the millisecond pulsar[21] PSR 1937 + 21 in the Vulpecula constellation. Its frequency stability is of the order of the stability of the better atomic frequency standards.[22] Of the 464 known radio pulsars,[23] PSR 1845-19 has the longest period, i.e., $p = 4.308$ s. We thus see that the period derivatives range over eight orders of magnitude, which is much greater than the four orders of magnitude occupied by the observed periods.

The secular variation of the period has superimposed upon it small but significant fluctuations that are probably random and unpredictable. In addition, many pulsars exhibit a step-like increase (glitch) in angular velocity, followed by slow relaxation. These period glitches are quite rare and, so far, have been observed only for 11 pulsars,[24,153] The largest glitch was observed in 1985 for pulsar PSR 0355 + 54. The relative reduction in period was[25] $\Delta p/p = 4.4\times 10^{-6}$ This pulsar is also remarkable in that its period was found to exhibit two glitches, the first being $\Delta p/p = 5.62\times 10^{-9}$ and was the smaller.[24] Eight large glitches were recorded for pulsar PSR 0833-45 in the Vela constellation, for which, in each case, the period fell by about 200 ns, which is very small in comparison with the rate of regular increase in the period, i.e., about 11 ns/day. The relative reduction $\Delta p/p$ for this pulsar is of the order of 2×10^{-6} and is found to be constant.[26–28] Pulsars PSR 1641-45, PSR 1325-43, PSR

 0038-5670/91/070555-17$01.00 © 1991 American Institute of Physics

2224 + 65, PSR 1737-30, and PSR 1823-13 had one large glitch each.[29–31] Three small glitches were recorded for the Crab pulsar with $\Delta p/p$ ranging between 10^{-9} and 4×10^{-8} (Ref. 32). Pulsars PSR 0525 + 21, PSR 0823 + 26, and PSR 1951 + 32 each showed one such glitch.[33,154] In each of these events the reduction in the period was accompanied by an increase in the period derivative $\dot{p}$. The increase then relaxed exponentially with a time constant ranging from a few days to a year. These time constants cannot be explained in terms of the normal viscosity of matter in neutron stars. The glitches in the rotational period and their slow relaxation suggest that neutron stars may have a superfluid component that is weakly coupled to the remainder of the star.

Experiments on the time-dependent dynamics of slowly-rotating superfluid He II lead to the same conclusion.[34–36] They revealed a deep analogy between the behavior of a pulsar after a period glitch and the behavior of superfluid He II when the rotation of its container was speeded up. Our aim in this review is to present recent results on the superfluidity and magnetic field of neutron stars.

Section 2 presents a description of the structure of neutron stars and discusses the superfluidity of their hadronic matter. Section 3 describes the drag of superfluid protons by superfluid neutrons in the superfluid core of the neutron star. Section 4 constitutes the main part of our review and is devoted to the generation of magnetic fields in pulsars by superfluid currents. Section 5 discusses an explanation of period glitches in terms of the motion of a lattice of quantized neutron vortex lines.

2. SUPERFLUIDITY OF HADRONIC MATTER

In 1932, L. D. Landau suggested for the first time that superdense cores could be formed in massive stars that have exhausted their internal energy reserves.[37] W. Baade and F. Zwicky[38] then predicted the possible existence of neutron stars in supernova remnants. Relativistic calculations on such superdense stellar configurations consisting of a degenerate perfect gas of neutrons were first performed by J. Oppenheimer and G. Volkoff.[39] This led to the concept of neutron stars consisting mostly of neutrons with mass of the order of one solar mass $M_\odot$ and radius of the order of 10 km. The mean density in the interior of such stars was predicted to be of the order of the nuclear density, i.e., $\rho_0 = 2.8\times10^{14}$ g/cm^3.

After the discovery of many new types of baryons, the theory of superdense stellar configurations was re-examined and developed further by V. A. Ambartsumayan and G. S. Saakyan.[40,41] They found that, as the density rose, different hyperons should successively appear and grow in number in the degenerate gas. Superdense stellar configurations consisting of a real baryon gas were discussed in Refs. 42 and 43. These investigations showed that neutron stars had a maximum mass of approximately $2M_\odot$. At present, the mass of pulsar PSR 1913 + 16, which is part of a binary system, is the most accurately known. It amounts to 1.43 $M_\odot$.

Our inadequate understanding of the structure of neutron stars arises from the sensitivity of this structure to the form of the equation of state of nuclear matter for densities in excess of nuclear density $\rho_0 = 2.8\times10^{14}$ g/cm^3. This equation has not as yet been adequately investigated. Difficulties with understanding the equation of state at such densities are due to uncertainties about the nucleon-nucleon interaction and the complexity of calculations of ground-state energy in many-particle theory.

2.1. Structure of neutron stars

The following picture of the internal structure of neutron stars is now generally accepted.

(a) The crust of a neutron star consists of the inner Aen-phase and the outer Ae-phase.[5] The latter consists mostly of ^{56}Fe nuclei and a degenerate gas of free electrons. Because of the electrostatic repulsion between them, iron nuclei form a body-centered crystal lattice, thus creating the solid outer crust of the neutron star. The density of matter in the Ae-phase ranges from 10^4 to 4.3×10^{11} g/cm^3.

The Aen-phase contains all the neutron-enriched nuclei forming another crystal lattice and the degenerate gases of free relativistic electrons and free neutrons.[5] The density of matter in the Aen-phase ranges from 4.3×10^{11} to 2.4×10^{14} g/cm^3. The total thickness of the crust is of the order of 1 km (Ref. 44).

(b) The nuclei disintegrate at densities of the order of the nuclear density $\rho_0 \approx 2.8\times10^{14}$, and the npe-phase is formed. It consists of a homogeneous mixture of neutron, proton, and electron fluids.[5] The proton and electron densities are equal because of local neutrality, and amount to a few per cent of the neutron density.

Hyperons and muons are produced in the central part of the star at densities of the order of 10^{15} g/cm^3. A hyperon core is thus seen to appear at the center of the star and contains hyperons, nucleons, muons, and electrons. For configurations with high central densities ρ_c, most of the stellar mass is localized in this core.[5] The radius of the core is of the order of 10 km.

(c) A. B. Migdal has shown[45] that, when the density ρ is high enough, the boson vacuum is restructured in the nucleon medium, and this leads to a phase transition in which the pion condensate is formed. The condensate produces a significant softening of the equation of state of the neutron star[45,46] and thus affects such important integral parameters of neutron stars as their mass, radius, and moment of inertia. The appearance of the pion condensate is accompanied by a substantial increase in the rate of cooling of the neutron star produced in the supernova explosion.[47–49] Several models rely on the van der Waals equation of state, which leads to a first-order phase transition, i.e., a density jump occurs in the interior of the neutron star and may lead to the release of energy of the order of the energy of the supernova explosion.[50,51]

A core containing the pion condensate can thus appear at the center of the star. The authors of Ref. 52 use the developed pion condensate model (DPCM),[53] modified[54] to allow for the electric charge, together with the Bethe-Johnson equation of state[55] in which the npe-phase ends at density $\rho_1 = 8.45\times10^{14}$ g/cm^3 and the core containing the pion condensate begins for density $\rho_2 = 1.28\times10^{15}$ g/cm^3. The integral parameters of the neutron star with central density $\rho_c = 3.45\times10^{15}$ g/cm^3 are as follows: mass $M = 1.41M_\odot$, stellar radius $R = 9.31$ km, and radius of the core containing the pion condensate $R_c = 6.2$ km. For comparison, we reproduce the integral parameters of an ordinary neutron star described by the Bethe-Johnson equation of state for central density $\rho_c = 3\times10^{15}$ g/cm^3:$M = 1.65M_\odot$ and $R = 9.6$ km (Ref. 56).

2.2. Superfluidity of nuclear matter

A new stage in the investigation of the internal structure of neutron stars and the structure of atomic nuclei began with the advent of the microscopic theory of superfluidity.[57] N. N. Bogolyubov pointed out the possibility of superfluid nuclear matter[58] and A. Bohr, B. Mottelson, and D. Pines considered superfluid states in atomic nuclei.[59] The theory of superconducting-type pair correlations was developed independently by S. T. Belyaev[60] and by V. G. Solov'ev,[61] and was found to explain many nuclear properties.

The basic ideas and methods of the microscopic theory of superconductivity were then used to analyze the internal structure of neutron stars. A. B. Migdal investigated the equation of state of the neutron fluid and was led to the possibility of superfluidity in neutron stars.[62] V. L. Ginzburg and D. A. Kirzhnits[63] used the analogy with rotating He II to suggest the possibility of a certain configuration of vortex lines in a rotating neutron superfluid. They also estimated that the neutron energy gap in the $^1S_0$-state was of the order of a few MeV. Similarly, the strong interaction between protons gives rise to Cooper pairs and to a charged proton condensate in the npe-phase.[64] On the other hand, electrons form a normal degenerate Fermi gas.

Studies of the superfluidity of hadronic matter became more intensive following the discovery of pulsars and of the angular velocity glitches. In particular, anisotropic pairing of neutrons in the core of a neutron star[67] was investigated[65,66] by analogy with anisotropic pairing in superfluid ^{3}He. The change in the character of pairing is due to the fact that the $^1S_0$ interaction between neutrons becomes repulsive at nuclear densities, and singlet pairing is disrupted. However, the $^3P_2$–$^3F_2$ tensor interaction in this density range leads to an effective attraction and to triplet pairing.[68] The effect of proton superconductivity on the magnetic-field configuration and decay was examined in Refs. 69 and 70. The coupling between the solid crust and the superfluid core was studied in Refs. 71. The following picture has emerged from these investigations:

(a) For densities in the range $4.6\times10^{11} < \rho < 1.6\times10^{14}$ g/cm^3, free neutrons in the Aen-phase form a superfluid containing $^1S_0$ pairs. The rotation of the star then ensures that a structure consisting of quantized vortex lines parallel to the axis of rotation appears in this fluid. The cores of the vortex lines, in which the condensate function vanishes, can become attached to the atomic nuclei in the crust (this is the so-called pinning) or they can pass between the nuclei. The maximum neutron gap is $\Delta_{2\max} = 1.7$ MeV (Ref. 72).

(b) For densities $1.6\times10^{14} < \rho < 1.4\times10^{15}$ g/cm^3 in the npe-phase, the neutron superfluid is more likely to consist of $^3P_2$ pairs, and a system of vortices is again formed. The maximum neutron gap is $\Delta_{2\max} = 0.15$ MeV (Ref. 73).

(c) The proton fluid in the npe-phase becomes superconducting for densities in the range $2.4\times10^{14} < \rho < 7.8\times10^{14}$ g/cm^3. The protons pair off in the $^1S_0$-state and constitute a type II superconductor in which a mixed-state vortex structure is established, i.e., the magnetic field penetrates the interior in the form of quantized vortex lines with flux $\Phi_0 = 2\times10^{-7}$ G·cm^2. The maximum gap is[72] $\Delta_{1\max} = 0.3$ MeV. The dependence of the proton gap on the density is also calculated in Ref. 74.

Different authors have used different methods and different nucleon interaction potentials to calculate the gap Δ as a function of the density of matter. These potentials included the Reid potential,[75] the one-pion Gaussian exchange potential,[76] the Omura potential,[77] and so on. The results reported by the different workers are qualitatively very different. The reason for this is that theoretical studies are still continuing with the view to improving the superfluid parameter values of hadronic matter.[78,79] Values of the function Δ calculated by different workers are compared in the figure.

In the publications cited above, the energy gap Δ was calculated at zero temperature. However, we know that Δ decreases with increasing temperature, and vanishes at a certain critical temperature T_c at which the medium goes over to the normal state. The question of the existence of superfluid neutrons and protons in a neutron star is thus effectively reduced to the comparison of the critical temperatures with the temperature in the stellar interior. The critical temperature T_c is usually estimated from the BCS formula $k_B T_c = 0.57\ \Delta$. According to Refs. 72 and 73, for protons

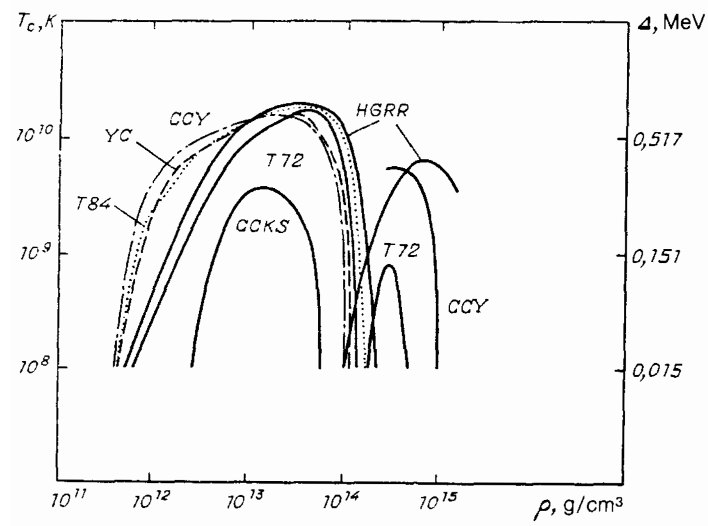

FIG. 1. Superfluidity in the Aen- and npe-phases of a neutron star. CCY–proton gap as a function of density.[74] The other curves show the neutron gap as a function of density: HGRR–Ref. 7, YC–Ref. 77, T72–Ref. 68, T84–Ref. 78, CCKS–Ref. 79. The critical temperature T_c as a function of density is also shown. The figure is based on Ref. 155.

$T_{c1} = 2\times 10^9$ K and for neutrons $T_{c2} = 10^{10}$ K ($^1S_0$-pairing) and $T_{c2} = 9\times 10^8$ K ($^3P_2$-pairing). Standard cooling calculations have shown that the internal temperature T approaches 10^8 K after a few hundred years following the birth of the star.[80-82]

The internal temperature of pulsars, including some very young pulsars, is thus found to be lower than the characteristic critical temperatures of neutron and proton superfluid condensates, which may be regarded as a convincing argument in favor of the existence of both neutron and proton superfluidity in the nucleon-nuclear phase.

(d) Neutron stars with a "soft" equation of state have a core consisting of a superconducting negative-pion condensate.[53] We shall show below that a strong magnetic field is generated in the npe-phase. This situation gives rise to the following question: is it possible for the magnetic field induced in the npe-phase to penetrate the core of the neutron star, which contains the superconducting pion condensate, and, if the answer is in the affirmative, what is the structure of the magnetic field in the star?

To answer this question, we must take into account the pion-nucleon interaction in the meson σ-model, which leads to the following important changes in the physical picture.[83] First, the attractive P-wave pion-nucleon interaction transforms the pion condensate into an inhomogeneous state with characteristic momentum $\mathbf{k}\neq 0$ and, second, in addition to the negative-pion condensate there is also the condensate of positive pions in the S-state in the form of a bound state of a proton and a neutron hole. We note that the presence of the positive-pion condensate gives rise to an additional electric current.

The superconducting properties of the inhomogeneous pion condensate were discussed in Ref. 83 in the σ-model.[53] The critical field H_c for the destruction of the superconductivity of the pion condensate was found on the assumption that it was a type I superconductor. The lower critical field H_{c1} was estimated for a type II superconductor on the assumption that the mixed state of the system had a vortex-line structure.

The behavior of the inhomogeneous pion condensate in a magnetic field near the condensation threshold was also investigated in Ref. 84 in which the Lagrange function of the system was expanded in terms of the amplitude of the condensate field. It was shown that the pion condensate was a type II superconductor with $\delta \gg 1$ in which the mixed state had a laminar (layered) structure. However, this method cannot be employed for densities much above the threshold pion density ρ_1. We also note that the density range in which this analysis is valid is not encountered in a neutron star because of the density jump at negative-pion condensation.

We shall show later that, in the σ-model, the negative-pion condensate is a type II superconductor with a laminar structure of the mixed state.

2.3. Vortex structure of the neutron fluid as a consequence of rotation

An asymetric lattice of quantized vortex lines parallel to the axis of rotation is formed in a rotating superfluid. This lattice rotates as a whole around the axis of rotation, thus simulating rigid rotation.[85] Consequently such vortex lattices are formed in the neutron superfluid in the Aen- and npe-phases. Each neutron vortex line is characterized by a circulation quantum given by[63]

$$\varkappa_2 = \frac{\pi\hbar}{m_2}, \tag{2.1}$$

where $\hbar = 1.054\times 10^{-27}$ erg·s is Planck's constant and m_2 is the neutron mass. The radius of the normal neutron core of each vortex is equal to the coherence length of the neutron fluid and is given by

$$\xi_2 = \frac{(3\pi^2)^{1/3}\hbar^2}{2m_2^{4/3}}\frac{\rho_2^{1/3}}{\Delta_2}, \tag{2.2}$$

where ρ_2 is the total neutron mass density. The outer radius b of the neutron vortex and the vortex density N_2 are given by the following expressions:

$$N_2 = \frac{2\Omega}{\varkappa_2}, \quad b = \left(\frac{\varkappa_2}{2\pi\Omega}\right)^{1/2}; \tag{2.3}$$

where Ω is the angular velocity of the neutron star. The number of vortex lines is thus seen to be determined by the angular velocity. Consequently, the number of vortices should decrease as rotation slows down. However, within a certain interval of time, the number of vortices in the star may be greater than the equilibrium value corresponding to the new Ω. A metastable state is then created in the vortex structure[86] and corresponds to minimum local free energy. This metastable state vanishes when the excess vortices decay and transfer their angular momentum to the solid crust. This spontaneous speeding up of the rotation of the freely rotating vessel containing the superfluid liquid has actually been observed experimentally.[87]

For the Crab pulsar, the equilibrium values are $N_2 = 2\times 10^5$ cm^{-2} and $b = 10^{-3}$ cm ($\Omega = 191$ s^{-1}), whereas for the millisecond pulsar PSR 1937 + 21, the values are $N_2 = 4\times 10^6$ cm^{-2} and $b = 2\times 10^{-4}$ cm ($\Omega = 4\times 10^3$ s^{-1}). The coherence length is $\xi_2 = 10^{-12}$ cm.

The superfluid neutrons in the vortex rotate around the normal core with velocity

$$v = \frac{\varkappa_2}{2\pi r}, \tag{2.4}$$

where r is the distance from the vortex center. The internal energy per unit length (linear tension) of a vortex line is given by[85]

$$E_{\text{B}} = \frac{\rho_2\varkappa_2^2}{4\pi}\cdot\ln\left(\frac{b}{\xi_2}\right). \tag{2.5}$$

Let us now determine the shape of a neutron vortex line in a spherical neutron star.[88] The symmetry of the problem near the equatorial plane ensures that the vortex lines are straight and perpendicular to this plane. By writing down the free energy of an infinitesimally thin layer near the equatorial plane, and then minimizing it, we find the velocity distribution in this plane. The velocity of the superfluid neutrons in a vortex is as before given by (2.4), and the internal energy is given by (2.5). The set of vortex lines participates as a whole in the rigid-body rotation.

We note that the internal energy (2.5) is a logarithmic function of the ratio b/ξ_2. It is therefore independent of the latitude of the star and can be regarded as constant. Next, the requirement that vortex lines leaving the equatorial plane must remain in the same ρ, z plane (this follows from the axial symmetry of the problem) ensures that the macroscopic velocity of the vortices is given by $\vec{v} = \vec{\Omega} \times \vec{\rho}$ at all points (ρ is the distance from the axis of rotation).

We must now find the shape of a vortex line $\rho(z)$ from the condition for minimum total energy of the neutron fluid per vortex line. The result is:[88]

$$\rho^2(z) + \frac{\varepsilon(\Omega)}{(1+\rho'^2)^{1/2}} = \text{const} + \frac{\Gamma}{\pi\Omega}\cdot\ln\rho(z), \tag{2.6}$$

where

$$\varepsilon(\Omega) = \frac{\varkappa_2}{2\pi\Omega}\ln\left(\frac{\varkappa_2}{2\pi\Omega\xi_2^2}\right), \quad \Gamma = 2\pi\Omega\rho_{\min}^2, \quad \rho' = \frac{d\rho}{dz}, \tag{2.7}$$

and $\rho_{\min}$ is the coordinate of the intersection of the vortex line with the equatorial plane. If we determine the constant of integration in (2.6) from the boundary condition that the vortex line must be perpendicular to the surface of the sphere,[89] and find $\rho_{\min}$ from the condition $\rho'(z) = 0$, we find that the displacement of the line, $\Delta\rho = \rho_0 - \rho_{\min}$, from a straight line is given by[88]

$$\Delta\rho = \left[\left(1 - \frac{|z_0|}{R_1}\right)\frac{\varepsilon(\Omega)}{2}\right]^{1/2}, \tag{2.8}$$

where z_0 and ρ_0 are the coordinates of the vortex line on the surface of the sphere and R_1 is the radius of the *npe*-phase. Since $\varepsilon(\Omega)$ is a sufficiently small quantity, the neutron vortices in the npe-phase of the rotating star are always parallel to the axis of rotation except for a small layer in the immediate vicinity of the surface in which they become curved and run outward in the perpendicular direction. The displacement $\Delta\rho$ is zero for the vortex line crossing the axis of rotation and is a maximum for the line located at a distance of the order of R_1 from the axis of rotation ($\Delta\rho_{\max} \sim 10^{-3}$cm).

The rotation of a superfluid sphere was also investigated in Ref. 90 in which it was found that the lower critical velocity is given by

$$\Omega_{c1} = \frac{3\hbar}{4m_2 R_1^2}\cdot\left[\ln\left(\frac{2R_1}{\xi_2}\right) - 1\right]. \tag{2.9}$$

The magnitude of Ω_{c1} for a sphere is greater by a factor of about 1.5 than for a cylinder of the same radius. Typically, for a neutron star $R_1 = 10$ km and $\xi_2 = 10^{-12}$ cm, so that if we substitute these values in the above expression, we obtain $\Omega_{c1} = 10^{-14}\ \text{s}^{-1}$.

The width of the irrotational region containing no vortices is given by:[90]

$$R_1 - \rho_1 = \left[\frac{15}{32}\cdot\frac{\varkappa_2}{\pi\Omega}\cdot\ln\left(\frac{b}{\xi_2}\right)\right]^{1/2}. \tag{2.10}$$

For angular velocities $\Omega = 1\ \text{s}^{-1}$ and $\Omega = 191\ \text{s}^{-1}$, the widths of the irrotational region are 8×10^{-2} and 5×10^{-3} cm, respectively. We therefore conclude that a well-developed neutron vortex structure corresponds to values of Ω typical for pulsars.

3. DRAG EFFECT IN THE SUPERFLUID CORE OF A STAR

So far, the superfluid neutron condensate and the superfluid proton condensate in the electron-baryon plasma of the npe-phase have been regarded as strictly noninteracting. However, the strong interaction between protons and neutrons ensures that they transform into quasiparticles with effective masses m_1^* and m_2^*. The motion of a neutron quasiparticle is thus seen to transport not only the neutron mass, but the proton mass as well. Cooper pairs of neutrons and of protons are the bound states of Fermi quasiparticles whose properties remain practically unaltered as superfluidity is established. Consequently, the superfluid motion of neutrons must be accompanied by the transport of proton mass (this is the so-called drag of superfluid protons by superfluid neutrons). Since protons are charged, the superfluid motion of neutrons gives rise to an electric current, i.e., the drag current.[91]

We note that proton-neutron Cooper pairs are not produced because the difference between the chemical potentials of neutrons and protons in the npe-phase is large.

3.1. Microscopic theory of superfluidity in a two-component Fermi system

Systems in which there are two types of condensate and, consequently, two types of superfluid motion, have been the subject of intensive investigation in recent years. An example of a system of this type is the solution of He^3 in He^4 below the phase transition of He^3 to the superfluid state. The equations of the three-velocity hydrodynamics, which describe the properties of this solution, were obtained by I. M. Khalatnikov.[92,93] A. F. Andreev and E. P. Bushkin[94] have in addition taken into account the drag of the He^3 condensate by the He^4 condensate, and showed that each of the superfluid motions is accompanied by the transport of both components of the solution.[94]

The npe-phase of the neutron star is another system with two superfluid condensates. The microscopic theory of superfluidity in a neutron-proton Fermi system with interaction between the components was constructed in Refs. 95 and 96. If we use the expression for the total Hamiltonian for this system[95] and the mathematical formalism of anomalous Green functions,[97,98] we obtain near the lower critical temperature the solution of the set of equations for the temperature Green functions of protons and neutrons.[95] This procedure presupposes that the coupling constants in the total Hamiltonian are small, since the graphical summation employed in this method does not take into account diagrams that lead to third-order terms in the coupling constants in these equations.

Next, using the standard method,[99] we obtain the Ginzburg–Landau equations for the two-component superfluid Fermi system[96]

$$\begin{gathered}
\frac{1}{4m_1'}\cdot\left[-i\hbar\nabla - \frac{2e}{c}(A + A')\right]^2\psi_1 \\
+ (\alpha_1 + \alpha_1'|\psi_2|^2)\psi_1 + \beta_1|\psi_1|^2\psi_1 = 0, \\
\mathbf{j}_e = \frac{ie\hbar}{2m_1'}\cdot(\psi_1\nabla\psi_1^* - \psi_1^*\nabla\psi_1) - \frac{2e^2}{cm_1'}\cdot(A + A')|\psi_1|^2, \\
\frac{1}{4m_2'}\cdot\left[-i\hbar\nabla + A_1\right]^2\psi_2 + (\alpha_2 + \alpha_1'|\psi_1|^2)\psi_2 + \beta_2|\psi_2|^2\psi_2 = 0, \\
\mathbf{j}_2 = \frac{i\hbar m_2}{2m_2'}(\psi_2\nabla\psi_2^* - \psi_2^*\nabla\psi_2) + \frac{m_2}{m_2'}A_1|\psi_2|^2,
\end{gathered} \tag{3.1}$$

where m_1' and m_2' are the proton and neutron masses renormalized by the interaction, $\mathbf{j}_2$ is the mass current density of the superfluid neutrons, $\mathbf{j}_e$ is the superfluid proton current density, $\mathbf{A}'$ is the effective vector potential due to the drag of superfluid protons by superfluid neutrons,

$$\mathbf{A}' = \frac{i\hbar m_1' c M_1}{8em_1C_1C_2}(\psi_2\nabla\psi_2^* - \psi_2^*\nabla\psi_2), \qquad (3.2)$$

and $\mathbf{A}_1$ is defined by

$$\mathbf{A}_1 = \frac{i\hbar m_2' M_1}{4m_1C_1C_2}(\psi_1\nabla\psi_1^* - \psi_1^*\nabla\psi_1 + \frac{4ie}{\hbar c}\mathbf{A}|\psi_1|^2); \qquad (3.3)$$

in which ψ_1 and ψ_2 are the condensate wave functions of protons and neutrons, given by

$$\psi_1 = \left(\frac{n_1}{2}\right)^{1/2} e^{i\varphi_1}, \quad \psi_2 = \left(\frac{n_2}{2}\right)^{1/2} e^{i\varphi_2}. \qquad (3.4)$$

The coefficients α_1' and M_1 are proportional to the square of the coupling constant. In the absence of interaction between the components, we have $\alpha_1' = 0$, $M_1 = 0$, $\mathbf{A}_1 = 0$, $\mathbf{A}' = 0$, the first pair of equations in (3.1) transforms into the Ginzburg–Landau equations for the resting superconductor,[100] and the second pair is analogous in form to the Ginzburg–Pitaevskiĭ equations of the phenomenological theory of superfluidity.[101]

If we define the superfluid velocities of protons and neutrons as follows:

$$\mathbf{v}_1 = \frac{\hbar}{2m_1}\nabla\varphi_1 - \frac{e}{m_1c}\mathbf{A}, \quad \mathbf{v}_2 = \frac{\hbar}{2m_2}\cdot\nabla\varphi_2, \qquad (3.5)$$

we can write the proton and the neutron mass current densities in the form

$$\mathbf{j}_1 = \frac{m_1}{e}\cdot\mathbf{j}_e = \rho_{11}\mathbf{v}_1 + \rho_{12}\mathbf{v}_2,$$
$$\mathbf{j}_2 = \rho_{21}\mathbf{v}_1 + \rho_{22}\mathbf{v}_2. \qquad (3.6)$$

It is clear from these expressions that some of the superfluid protons travel with the velocity of superfluid neutrons, and this produces the electric drag current.[91]

If we take the drag effect into account, the kinetic energy density assumes the form[96]

$$T_k = \frac{1}{2}\cdot(\rho_{11}\mathbf{v}_1^2 + 2\rho_{12}\mathbf{v}_1\mathbf{v}_2 + \rho_{22}\mathbf{v}_2^2). \qquad (3.7)$$

This expression will be used later when we investigate the generation of magnetic fields in pulsars.

The Ginzburg–Landau equations that we have obtained for the two-component superfluid Fermi system (3.1) are strictly valid only in a narrow range near the lower critical temperature T_{c1} (the proton critical temperature). We shall show later that the drag effect will also occur for temperatures $T\to 0$.

3.2. Three-velocity magnetohydrodynamics of superfluid solutions

The properties of the electron-baryon plasma in the npe-phase for $T\to 0$ should satisfy the equations of three-velocity magnetohydrodynamics with two superfluid and one normal velocity.

The analysis of conservation laws given in Refs. 92 and 94 shows that the complete set of equations of three-velocity magnetohydrodynamics has the following form in the absence of dissipation:[102]

$$\dot\rho_1 + \mathrm{div}(\rho_1\mathbf{v}_n + \mathbf{p}_1) = 0, \quad \dot\rho_2 + \mathrm{div}(\rho_2\mathbf{v}_n + \mathbf{p}_2) = 0,$$
$$\dot j_i + \partial\Pi_{ik}/\partial x_k = 0, \quad \dot S + \mathrm{div}(S\mathbf{v}_n) = 0,$$
$$\dot\rho_e + \mathrm{div}(\rho_e\mathbf{v}_n) = 0, \quad \dot{\mathbf{v}}_e + \frac{\nabla P_e}{\rho_e} = -\frac{e\mathbf{E}}{m_e} - \frac{e}{c}[\mathbf{v}_e\mathbf{B}],$$
$$\dot{\mathbf{v}}_1 + \nabla(\mu_1 - \frac{1}{2}\mathbf{v}_n^2 + \mathbf{v}_n\mathbf{v}_1) = \frac{e}{m_1}\cdot\mathbf{E} + \frac{e}{c}[\mathbf{v}_1\mathbf{B}], \qquad (3.8)$$
$$\dot{\mathbf{v}}_2 + \nabla(\mu_2 - \frac{1}{2}\mathbf{v}_n^2 + \mathbf{v}_n\mathbf{v}_2) = 0,$$
$$\mathrm{curl}\,\mathbf{v}_2 = 0, \quad \mathrm{curl}\,\mathbf{v}_1 = -\frac{e}{m_1c}\cdot\mathbf{B};$$

where ρ_1, ρ_2, and ρ_e are the proton, neutron, and electron mass densities, $\mathbf{v}_1$, $\mathbf{v}_2$, and $\mathbf{v}_n$ are the velocities of the two superfluid and one normal motions, m_e, $\mathbf{v}_e$ are the mass and the velocity of the electrons (the latter is equal to the velocity of normal motion $\mathbf{v}_n$), S and $\mathbf{j}$ are the entropy and momentum per unit volume, and μ_1, μ_2, $\mathbf{p}_1$, $\mathbf{p}_2$ are the chemical potentials and relative momenta of superfluid protons and neutrons. It is assumed in (3.8) that $m_e^* \sim m_e \ll m$ where m_e^* is the effective mass of the electron.

The momentum flux tensor is given by[102]

$$\Pi_{ik} = (\rho_1 + \rho_2)v_{ni}v_{nk} + (p_{1i} + p_{2i})v_{nk} + (p_{1k} + p_{2k})v_{ni} + P\delta_{ik}$$
$$+ p_{1k}(v_{1i} - v_{ni}) + p_{2k}(v_{2i} - v_{ni}) - \frac{1}{4\pi}(H_iH_k - \frac{1}{2}\cdot\delta_{ik}H^2), \qquad (3.9)$$

where $p = -\varepsilon + \mu_1\rho_1 + \mu_2\rho_2 + \mu_e\rho_e + TS$ is the pressure. The electric and magnetic fields are given by the Maxwell equations that augment (3.8).

Following the method put forward in Ref. 94, and using the basic conservation law with allowance for the magnetic field and the laws of thermodynamics, it is readily shown that the characteristic superfluid condensate quantities ρ_{11}, ρ_{12}, ρ_{22} are given by

$$\rho_{11} = \frac{m_1^2}{m_1^*}n_1, \quad \rho_{12} = \rho_{21} = \frac{m_1(m_1^* - m_1)}{m_1^*}n_1,$$
$$\rho_{22} = \rho_2 - (m_1^* - m_1)n_{1n} - \frac{m_1(m_1^* - m_1)}{m_1^*}n_1; \qquad (3.10)$$

where n_1 and n_{1n} are the densities of the superfluid and normal protons, and m_1 and m_1^* are, respectively, the "bare" and effective proton masses. The quantities $\rho_{\alpha\beta}$ $(\alpha,\beta = 1,2)$ are the analogs of the density of the superfluid part in two-velocity hydrodynamics.

According to the BCS theory, the superfluid velocities $\mathbf{v}_1$ and $\mathbf{v}_2$ are microscopically expressed in terms of the phase angles φ_1 and φ_2 of the condensate wave functions of protons and neutrons, as follows:

$$\mathbf{v}_1 = \frac{\hbar}{2m_1}\cdot\nabla\varphi_1 - \frac{e}{m_1c}\mathbf{A}, \quad \mathbf{v}_2 = \frac{h}{2m_2}\nabla\varphi_2. \qquad (3.11)$$

The fact that (3.11) contains the neutron mass m_2, and not the effective mass of the Fermi excitation, ensures that the superfluid motion of the neutrons is potential.

Let us suppose to begin with that $\mathbf{v}_2 = \mathbf{v}_n = 0$. According to the BCS theory, the mass current density of superfluid protons is then given by

$$\mathbf{j}_1 = \frac{m_1}{e}\left(\frac{e\hbar n_1}{2m_1^*}\nabla\varphi_1 - \frac{e^2 n_1}{m_1^* c}\mathbf{A}\right) = \rho_{11}\mathbf{v}_1. \quad (3.12)$$

The mass current density of superfluid neutrons can be shown to be given by the following expression if we use the total mass current density given in Ref. 102:

$$\mathbf{j}_2 = m_1\left(1 - \frac{m_1}{m_1^*}\right)\left(\frac{\hbar}{2m_1}\nabla\varphi_1 - \frac{e}{m_1 c}\mathbf{A}\right)n_1 = \rho_{12}\mathbf{v}_1. \quad (3.13)$$

It is thus clear that some of the superfluid neutrons will travel with the velocity of the superfluid protons.

Next, let us put $\mathbf{v}_1 = \mathbf{v}_n = 0$. Using the method proposed in Ref. 103, we then find that the energy $\varepsilon(\mathbf{p})$ of the proton quasiparticle is given by the following expression in the approximation that is linear in $\mathbf{v}_2$ (Ref. 104):

$$\varepsilon(\mathbf{p}) = \frac{1}{2m_1^*}(\mathbf{p} - \frac{e}{c}\mathbf{A}')^2,$$
$$\mathbf{A}' = \mathbf{A} - \frac{c}{e}(m_1^* - m_1)\mathbf{v}_2. \quad (3.14)$$

The interaction between the proton and neutron condensates thus ensures that the true vector potential $\mathbf{A}$ is replaced with $\mathbf{A}'$. The mass current density $\mathbf{j}_1$ can therefore be readily obtained from the London formula $\mathbf{j}_e = -(e^2 n_1/m_1^* c)\mathbf{A}'$. We have

$$\mathbf{j}_1 = \frac{m_1(m_1^* - m_1)}{m_1^*}n_1\mathbf{v}_2 - \frac{em_1 n_1}{m_1^* c}\mathbf{A} = \rho_{12}\mathbf{v}_2 - \frac{m_1 e n_1}{m_1^* c}\mathbf{A}. \quad (3.15)$$

Consequently, some of the superfluid protons will travel with the neutron velocity $\mathbf{v}_2$.

The total mass current density operator is

$$\mathbf{j} = \rho_2\mathbf{v}_2 + \sum_{\mathbf{p}}(\mathbf{p} - \frac{e}{c}\mathbf{A})n_{\mathbf{p}}, \quad n_{\mathbf{p}} = \sum_{\alpha}\hat{a}^+_{\mathbf{p}\alpha}\hat{a}_{\mathbf{p}\alpha}, \quad (3.16)$$

where $\hat{a}^+_{p\alpha}$, $\hat{a}_{p\alpha}$ are the proton quasiparticle creation and annihilation operators and α is the spin index. Transforming this mass current operator, and using the explicit form of the electric current density operator,[102] we find that the total mass current density is

$$\mathbf{j} = \rho_2\mathbf{v}_2 - (m_1^* - m_1)n_{1n}\mathbf{v}_2 - \frac{e}{c}n_1\mathbf{A}, \quad (3.17)$$

where $n_{1n} = n - n_1$ and ρ_2 is the neutron mass density. The mass current density of superfluid neutrons can now be found from (3.15) and (3.17):

$$\mathbf{j}_2 = \rho_{22}\mathbf{v}_2 - \frac{e}{m_1 c}\rho_{12}\mathbf{A}. \quad (3.18)$$

Finally, let us suppose that $\mathbf{v}_1 = \mathbf{v}_2 = \mathbf{A} = 0$. The problem then reduces to the case examined in Ref. 94 for which the mass current densities are given by

$$\mathbf{j}_1 = (\rho_1 - \rho_{11} - \rho_{12})\mathbf{v}_n = \rho_1^{(n)}\mathbf{v}_n,$$
$$\mathbf{j}_2 = (\rho_2 - \rho_{22} - \rho_{21})\mathbf{v}_n = \rho_2^{(n)}\mathbf{v}_n. \quad (3.19)$$

According to (3.12)–(3.19), we may write

$$\mathbf{j}_1 = \rho_{11}\mathbf{v}_1 + \rho_{12}\mathbf{v}_2 + \rho_1^{(n)}\mathbf{v}_n,$$
$$\mathbf{j}_2 = \rho_{22}\mathbf{v}_2 + \rho_{21}\mathbf{v}_1 + \rho_2^{(n)}\mathbf{v}_n. \quad (3.20)$$

Consequently, in three-velocity magnetohydrodynamics, the density of the superfluid part is replaced by the three independent quantities ρ_{11}, ρ_{22}, ρ_{12}, the last of which describes the drag of both components of the solution by one of the superfluid motions. This effect is thus found to exist throughout the temperature range in which the neutron-proton liquid is superfluid.

The linearized set of magnetohydrodynamic equations, given by (3.8), is found to have wave-type solutions. The dispersion relations for these waves were obtained in Refs. 102 in which the velocities of the different acoustic oscillations were also calculated. It was shown that fourth sound can propagate in the neutron-proton superfluid.

4. MAGNETIC-FIELD GENERATION IN PULSARS

The generally accepted mechanism for the generation of the magnetic field in superdense stars is the contraction of the star with the simultaneous conservation of the initial magnetic flux.[105,106] Conservation of the magnetic flux is assured by the fact that the magnetic lines of force are "frozen-in" because of the very high conductivity of the stellar material. In the case of an isotropic contraction of an ordinary star, the magnetic field is proportional to r^{-2} or $\rho^{2/3}$ where r is the mean radius of the star and ρ is its density. Hence, for an initial magnetic field $B \sim 1$ G and initial value $r \sim 3\times10^{10}$ cm, we find that $B \sim 10^8$ G for $r_0 \sim 3\times10^6$ cm and $\rho_0 \sim 10^{12}$ G/cm^3 (Refs. 107 and 108). The initial field in a magnetic star can reach $10^3 - 10^4$ G, so that the field in a neutron star can reach $10^{11} - 10^{12}$ G (Ref. 108). It is assumed in all this that the stellar mass remains constant during the contraction process, i.e., $\rho r^3 =$ const. However, this mechanism ignores the dynamics of the contraction process. The contraction or collapse of an ordinary star after a supernova explosion is unavoidably accompanied by the turbulent motion of the material, and this leads to a sharp reduction in the electric conductivity σ of the stellar material[109] and a departure from the frozen-in character of the field. Moreover, some of the material may be ejected from the star during the supernova explosion, together with the accompanying magnetic field. These factors result in a substantial reduction in the final magnetic field strength and may even reduce it to zero. We must therefore consider other mechanisms for the generation of magnetic fields in neutron stars that are unrelated to the collapse phenomenon.

The ferromagnetism of neutrons was considered in Refs. 110–112 as the source of the magnetic field. Thermoelectric and thermomagnetic instabilities were used in Refs. 113 and 114 to obtain dipole magnetic fields of the order of $B \sim 10^{12}$ G.

We shall now consider superfluid proton currents as the source of the magnetic field of a neutron star.[115,116] This mechanism relies on the drag of superfluid protons by superfluid neutrons, and gives rise to magnetic fields of the order of $B \sim 10^{12}$ G.

4.1. London equation for a superfluid solution

Consider the superfluid core of a rotating neutron star in which the neutron superfluid forms a lattice of quantized vortices, and the charged component, which is rigidly coupled to the crust by the magnetic field, executes rigid rotation with velocity $\mathbf{v}_n = \vec{\Omega}\times\mathbf{r}$.

Using the definition given by (3.6), we can write the proton superfluid current density in the form

$$\mathbf{j}_e = \frac{e}{m_1}(\rho_{11}\mathbf{v}_1 + \rho_{12}\mathbf{v}_2) = \mathbf{j}_{11} + \mathbf{j}_{12}; \tag{4.1}$$

where $\rho_{11} + \rho_{12} = \rho_1$ and $\rho_{22} + \rho_{12} = \rho_2$ in which ρ_1 and ρ_2 are the proton and neutron mass densities, respectively, and the densities $\rho_{11}, \rho_{12}, \rho_{22}$ are given by (3.10).

We now define the drag coefficient as follows: $k = (m_1^* - m_1)/m_1 = \rho_{12}/\rho_{11}$. Under the conditions prevailing in the neutron star, $k = -0.5$. The current density $\mathbf{j}_{11}$ in (4.1) is the usual Meissner proton current and $\mathbf{j}_{12}$ is the drag current.

The magnetic field generated by the drag currents can be determined from the Maxwell equation

$$\text{curl } \mathbf{H} = \frac{4\pi}{c}\mathbf{j}_{12}. \tag{4.2}$$

The presence of the undragged superfluid protons ensures that the magnetic field $\mathbf{H}$ is different from the magnetic induction $\mathbf{B}$ which is determined by the equation

$$\text{curl } \mathbf{B} = \frac{4\pi}{c}(\mathbf{j}_{11} + \mathbf{j}_{12}). \tag{4.3}$$

Substituting (4.1) in (4.3), and recalling that[104]

$$\text{curl } \mathbf{v}_1 = -\frac{e}{m_1 c}\mathbf{B} + \varkappa_1 \mathbf{i}_1 \sum_i \delta(\mathbf{r} - \mathbf{r}_i), \tag{4.4}$$

$$\text{curl } \mathbf{v}_2 = \varkappa_2 \mathbf{i}_2 \sum_j \delta(\mathbf{r} - \mathbf{r}_j),$$

we obtain

$$\mathbf{B} + \lambda^2 \text{curl curl } \mathbf{B} = \Phi_0 \mathbf{i}_1 \sum_i \delta(\mathbf{r} - \mathbf{r}_i) + \Phi_1 \mathbf{i}_2 \sum_j \delta(\mathbf{r} - \mathbf{r}_j), \tag{4.5}$$

where the flux quanta Φ_0 and Φ_1 and the magnetic-field penetration depth λ are given by

$$\Phi_0 = \frac{\pi\hbar c}{e}, \quad \Phi_1 = \frac{m_1\rho_{12}}{m_2\rho_{12}}\Phi_0, \quad \lambda^2 = \frac{m_1^2 c^2}{4\pi e^2 \rho_{11}}. \tag{4.6}$$

Rotation can be taken into account in (4.5) by substituting $\mathbf{B}' = \mathbf{B} + 2m_1 c\vec{\Omega}/e$ (Refs. 117 and 118).

In the above expressions, $\mathbf{i}_1$ and $\mathbf{i}_2$ are unit vectors in the direction of the proton and neutron vortex lines, $\mathbf{r}_i$ and $\mathbf{r}_j$ are, respectively, the position vectors of the line centers, and $\varkappa_1 = \pi\hbar/m_1$ is the quantum of proton circulation. We thus obtain the London equation with two different possible vortex regions.

4.2. Free energy of a two-component system

To identify the vortex structures formed in the system, e.g., purely neutron, purely proton, or both together, we must establish which case is energetically the most favorable. We shall do this by writing down the free energy for the system in the form

$$F = \frac{1}{2}\int(\rho_{11}\mathbf{v}_1^2 + 2\rho_{12}\mathbf{v}_1\mathbf{v}_2 + \rho_{22}\mathbf{v}_2^2 + \rho^{(n)}\mathbf{v}_n^2)\mathrm{d}V + \frac{1}{8\pi}\int \mathbf{B}^2 \mathrm{d}V - \mathbf{M}\vec{\Omega}, \tag{4.7}$$

where $\rho^{(n)} = \rho - \rho_1 - \rho_2$ is the density of the normal component, ρ is the total density of the fluid and the angular momentum of the liquid is given by

$$\mathbf{M} = \int [\mathbf{r}(\mathbf{j} + \rho^{(n)}\mathbf{v}_n)]\mathrm{d}V, \quad \mathbf{j} = \mathbf{j}_1 + \mathbf{j}_2;$$

where the velocity $\mathbf{v}_1$ is determined from the Maxwell equation

$$\text{curl } \mathbf{B} = \frac{4\pi}{c}(\mathbf{j}_{11} + \mathbf{j}_{12} - \frac{e}{m_1}\cdot\rho_1\mathbf{v}_n). \tag{4.8}$$

Substituting for $\mathbf{v}_1$ in (4.7), we obtain

$$F = \frac{1}{8\pi}\cdot\int\{\mathbf{B}^2 + \lambda^2(\text{curl } \mathbf{B})^2\}\mathrm{d}V + \frac{1}{2}\cdot\int\rho_{22}'\{\mathbf{v}_2 - [\vec{\Omega}\mathbf{r}]\}^2\mathrm{d}V - \frac{1}{2}\cdot\int\rho[\vec{\Omega}\mathbf{r}]^2\mathrm{d}V, \tag{4.9}$$

where $\rho_{22}' = \rho_{22} - \rho_{12}^2/\rho_{11}$. The expression given by (4.9) can be used to determine the average values of $\mathbf{v}_2$ and $\mathbf{B}$. The average of $\mathbf{v}_2(r)$ is related to the mean density $N_2(\mathbf{r})$ of neutron vortices and is determined by minimizing the free energy

$$F_1 = F + \int N_2(r)F_{1\mathrm{B}}\mathrm{d}V, \tag{4.10}$$

where $\mathbf{F}_{1B}$ is the energy of a single neutron vortex. The averages are evaluated for distances much greater than the dimensions of the neutron vortices.

On the other hand, the average of the vector $\mathbf{B}(\mathbf{r})$ depends on the density $N_1(\mathbf{r})$ of the proton vortices, and is determined by minimizing the Gibbs potential:

$$F_2 = F - \frac{1}{4\pi}\int \mathbf{H}(\mathbf{r})\mathbf{B}(\mathbf{r})\mathrm{d}V, \tag{4.11}$$

where $\mathbf{H}(\mathbf{r})$ is the magnetic field strength produced by the given drag currents. When $N_1(\mathbf{r})$ is determined, the average is evaluated over distances much greater than the dimensions of the proton vortices. If b and λ are, respectively, the dimensions of the neutron and proton vortices, then b is always much greater than λ. This means that we can introduce a mean density of proton vortices even within the dimensions of a single neutron vortex.

4.3. Average $\mathbf{v}_2(\mathbf{r})$ or $N_2(\mathbf{r})$

Let us suppose that the star rotates with angular velocity Ω. From (4.9) we find that

$$F_{1\mathrm{B}} = (\Phi_0/4\pi\lambda^2)^2\ln\left(\frac{\lambda}{\xi_1}\right) + \rho_{22}'\frac{\varkappa_2^2}{4\pi}\ln\left(\frac{b}{\xi_2}\right) - \frac{1}{2}\rho_{22}'\varkappa_2\Omega(b^2 - \xi_2^2). \tag{4.12}$$

where ξ_1 is the proton coherence length. The first term is the magnetic energy of the neutron vortex line per unit length. The critical angular velocity Ω_{c1} can be found from (4.12). The value obtained in this way is not significantly different from that given by (2.9) in the absence of drag. It follows that the conclusion drawn in Section 2, namely, that a relatively dense lattice of neutron vortex lines is present, remains in force.

By minimizing F_1 we obtain the simple solution $\bar{v}_2(\mathbf{r}) = \vec{\Omega}\times\mathbf{r}$. This means that the main component of the npe-phase consists of neutrons in rigid rotation with angular velocity Ω and density N_2 given by (2.3).

The interaction between neutrons and protons does not therefore modify the average superfluid velocity of neutrons or the density of the neutron vortex lattice as compared with the case of a one-component rotating superfluid. If there are no proton vortices, the magnetic induction can be found from (4.5), and is given by

$$\mathbf{B} = -\frac{2m_1 c}{e}\vec{\Omega} + \Phi_1 \mathbf{i}_1 \sum_j K_0\left(\frac{|\mathbf{r}-\mathbf{r}_j|}{\lambda}\right). \tag{4.13}$$

Calculations then show that $B \sim 2\times 10^{-4}$ G.

The mean magnetic induction is thus seen to be almost zero. Rotation produces a dense net of neutron vortices, and the local magnetic field due to the drag currents associated with a neutron vortex line is almost completely compensated by the Meissner proton currents. However, this situation occurs only when the local field around a neutron vortex is less than the critical field H_{c1} necessary for the creation of a proton vortex. It will be clear later that this is not always the case and that a superdense net of proton vortices may surround the neutron line and lead to an increase in the mean magnetic induction of the neutron star.

4.4. Average of B(r) or N_1(r)

The strong local fields around a neutron vortex may be responsible for the appearance of proton vortex lines that are accompanied by a transition of some of the density of undragged protons to the normal state. This field is due to the proton drag current. By solving (4.2) near a neutron vortex, we obtain

$$H(r) = \frac{\Phi_1}{2\pi\lambda^2}\cdot\ln\left(\frac{b}{r}\right), \tag{4.14}$$

where r is the distance between the point of observation and the center of the line. Proton vortices can arise within a circle of radius r_1 which can be determined from the condition $H(r) = H_{c1}$. It is well known that

$$H_{c1} = \frac{\Phi_0}{6\pi\lambda^2}\cdot\ln\left(\frac{\lambda}{\xi_1}\right). \tag{4.15}$$

Substituting $H = H_{c1}$ and $r = r_1$ in (4.14), we obtain

$$r_1 = b\left(\frac{\lambda}{\xi_1}\right)^{-1/3|k|}. \tag{4.16}$$

It is clear from this that the dimensions of the region in which proton vortices are produced are quite sensitive to the drag coefficient k. In this region, we have $H > H_{c1}$, and the field H gives rise to the appearance of a set of such vortices with flux Φ_0. Consequently, the Gibbs free energy of the proton vortex structure is a minimum in the equilibrium state. Since the density of proton vortices in the region of radius $r_1 \gg \lambda$ is sufficiently high, and the maximum field strength at the center of the neutron vortex satisfies the condition $H_{c1} \leqslant H(\xi_1) < H_{c2}$, we can introduce the continuous distribution density $N_1(\mathbf{r})$ of proton vortices for an individual neutron vortex. The Gibbs free energy of a system of proton vortex lines can be written in the form

$$G = \int N_1(\mathbf{r})\varepsilon\, dV + 2\left(\frac{\Phi_0}{4\pi\lambda^2}\right)^2 \int N_1(\mathbf{r})N_1(\mathbf{r}')K_0\left(\frac{|\mathbf{r}-\mathbf{r}'|}{\lambda}\right) dV dV'$$
$$- \frac{1}{4\pi}\int \mathbf{H}(\mathbf{r})\mathbf{B}(\mathbf{r})\, dV, \tag{4.17}$$

where

$$\varepsilon = \left(\frac{\Phi_0}{4\pi\lambda^2}\right)^2 \ln\left(\frac{\lambda}{\xi_1}\right), \quad \mathbf{B}(\mathbf{r}) = \frac{\Phi_0}{2\pi\lambda^2}\mathbf{i}_1 \int N_1(\mathbf{r}')K_0\left(\frac{|\mathbf{r}-\mathbf{r}'|}{\lambda}\right) dV'. \tag{4.18}$$

The Gibbs potential is measured from the value corresponding to the absence of proton vortices $N_1(\mathbf{r}) = 0$. By varying (4.17) with respect to N_1 we obtain the equilibrium density

$$N_1(r) = \frac{H(r) - H_{c1}}{\Phi_0}. \tag{4.19}$$

Once we know $N_1(r)$, we can find the mean induction $\overline{B}$ evaluated over the entire npe-phase of the neutron star:

$$\mathbf{B} = \frac{\mathbf{i}_1}{\pi b^2}\int \Phi_0 N_1(r)\cdot 2\pi r\, dr = \mathbf{i}_1 \frac{k\Phi_0}{4\pi\lambda^2}\left(\frac{\lambda}{\xi_1}\right)^{-2/3|k|} \tag{4.20}$$

The magnetic moment of the neutron star turns out to be

$$\mathbf{M}_m = \frac{4}{3}\pi R_1^3 \bar{\mathbf{B}}\cdot\frac{3}{8\pi} = \frac{\pi R_1^3 \bar{\mathbf{B}}}{2}. \tag{4.21}$$

The coefficient $3/8\pi$ appears because the magnetization of a uniformally magnetized sphere is $\mu = 3\overline{B}/8\pi$. Substituting the usual values $\xi_1 = 10^{-12}$ cm and $\lambda = 10^{-11}$ cm, we obtain $|\overline{B}| \sim 10^{12}$ G and $|\overline{B}| \sim 10^{14}$ G in a neutron star and near a neutron vortex, respectively. The magnetic moments are of the order of 10^{30} G$\cdot$cm^3.

4.5. Dipole field of a vortex lattice

We showed in Section 2.3 that, in a spherical star, the neutron vortex lines in most of the npe-phase are parallel to the axis of rotation, and that it is only in the immediate vicinity of the surface that they become curved and run outward in the perpendicular direction. However, this discussion did not take into account the drag effect. When this is done, the shape of the vortex is again given by (2.6), and the line displacement $\Delta\rho$ is given by (2.8) except that the function $\varepsilon(\Omega)$ in (2.7) must be modified.[119] However, this change (which is due to the magnetic energy of the neutron vortex) is quite small. Consequently, the above conclusion about the shape of the vortices remains valid. The lines of force of the magnetic field and of the magnetic induction generated by proton drag have the same form. Consequently the lines of force cross the surface of the npe-phase in the radial direction. The dimensions of the region in which the magnetic induction differs from zero is of the order of 10^{-4}–10^{-5} cm in the models that we have considered, which is much less than the separation between the vortices and therefore less than the characteristic dimensions of the star. This means that, when we calculate the external magnetic field well away from the surface of the npe-phase, we may consider with good accuracy that the field on the surface is localized at points at which the neutron vortices touch the surface. Let us denote the spherical coordinates of these points by φ_j, θ_j and φ_j, $\pi-\theta_j$. In the limit in which $r_1 \leqslant b \leqslant R_1$, the radial component of the induction due to vortices on the surface of the sphere can be written in the form

$$B_r|_\Sigma = \frac{\Phi_0}{R_1^2}\sum_{\theta_j,\varphi_j}[\delta(\varphi-\varphi_j)\delta(\cos\theta-\cos\theta_j) - \delta(\varphi-\varphi_j)\delta(\cos\theta-\cos(\theta_j-\pi))]; \quad (4.22)$$

where the sum over φ_j and θ_j is evaluated within the ranges $0<\varphi_j\leqslant 2\pi$, $0<\theta_j\leqslant\pi/2$.

Using the completeness condition for the spherical functions, we can write (4.22) in the form

$$B_r|_\Sigma = \frac{\Phi_0}{R_1^2}\sum_{\theta_j,\varphi_j}\sum_{l=0}^{\infty}\sum_{m=-l}^{l} Y_{lm}(\theta,\varphi)\left(Y_{lm}(\theta_j,\varphi_j) - Y^*_{lm}(\theta_j-\pi,\varphi_j)\right). \quad (4.23)$$

The induction outside the star satisfies the Maxwell equations in vacuum and can be written in the form $B_e = -\operatorname{grad}\psi$. The expression for the scalar potential $\psi(r,\theta,\varphi)$ that corresponds to (4.23) is

$$\psi(r,\theta,\varphi) = \frac{\Phi_0}{R_1^2}\sum_{\theta_j,\varphi_j}\sum_{l=0}^{\infty}\sum_{m=-l}^{l}\frac{R_1^{l+2}}{l+1} Y_{lm}(\theta,\varphi)\left(Y_{lm}(\theta_j,\varphi_j) - Y^*_{lm}(\theta_j-\pi,\varphi_j)\right). \quad (4.24)$$

The component $B_r(r,\theta,\varphi)$ determined for $r=R_1$ is found to be identical with (4.23). We now replace summation in (4.24) with integration, and use the rule

$$\sum_{\theta_j,\varphi_j} \to \int \frac{R_1^2}{b^2}\cos\theta\, d\Omega. \quad (4.25)$$

This expression is based on the assumption that the number dN of neutron vortices running normally to the surface within the solid angle $d\Omega$ is $dN = R_1^2\cos\theta\, d\Omega/b^2$ and that the neutron vortex density is constant on the equatorial plane of the star. Integrating in (4.24) taking (4.25), into account we find that the scalar potential of the magnetic field is given by[119]

$$\psi(r,\theta) = \frac{\mu V\cos\theta}{r^2}; \quad (4.26)$$

where $V = 4\pi R_1^3/3$ is the volume of the star and μ is its specific magnetic moment (magnetization). We therefore conclude that the stellar magnetic field is similar to that of a dipole. This simple result relies on the assumption that the vortex lines are perpendicular to the surface and that their distribution density in the stellar interior is constant.

We must now consider the question whether the magnetic field induced in the npe-phase can penetrate the core of the neutron star, which contains the superconducting pion condensate. We shall do this by investigating the magnetic structure of the pion condensate. The total energy density of the superconducting state of the system in the σ-model[53] in an external magnetic field H can be written in the form[120]

$$\varepsilon_s(n,\theta,H) = \frac{3(3\pi^2)^{2/3}n^{5/3}}{10M} + \frac{1}{2}\cdot f_\pi^2(\mathrm{K}^2-\mu_\pi^2)\sin^2\theta + f_\pi^2 m_\pi^2(1-\cos\theta) + m\cdot n + \frac{n}{2}\{\mu_\pi - [(\mu_\pi\cos\theta)^2 + (g_A \mathrm{K}\sin\theta)^2]^{1/2}\} + \mathrm{H}^2, \quad (4.27)$$

where n and m are, respectively, the nucleon density and mass, μ_π and m_π are the chemical potential and mass of negative pions, $f_\pi = 0.675 m_\pi$ is the pion decay constant, θ is the chiral rotation angle, $g_A = 1.36$ is the axial weak interaction constant, $\mathbf{K} = \mathbf{k} - e\mathbf{A}(r)$, and bfk is the constant momentum of the pion condensate. Here and henceforth we use the system of units in which $\hbar = c = m_\pi = 1$, $e^2/4\pi = 1/137$. We note that the protons and neutrons in the core pion condensate are in the normal state and occupy the same Fermi sphere.

The superconducting pion current is given by[120]

$$\mathrm{j}_\pi = -\frac{\partial\varepsilon_s}{\partial \mathrm{A}} = ef_\pi^2\sin^2\theta\cdot\mathrm{K} - \frac{eng_A^2\sin^2\theta\cdot\mathrm{K}}{2[(\mu_\pi\cos\theta)^2 + (g_A\mathrm{K}\sin\theta)^2]^{1/2}} \quad (4.28)$$

in which the first term is the pure meson contribution to the current due to the negative-pion condensate and the second is the "nucleon" contribution due to the positive-pion current in the S state and the proton current. Substituting $\theta = \pi/2$ in (4.28), we obtain the following expression for the current in the case of a developed condensate:

$$\mathrm{j}_\pi = ef_\pi^2\mathrm{K} - eng_A\mathrm{K}/2|\mathrm{K}|. \quad (4.29)$$

We note that, when $\theta=\pi/2$, the charge density of the nucleon subsystem in terms of the bare particles is $-en/2$ (Ref. 53), so that the velocity of the charged nucleon matter is $g_A\mathbf{K}/|\mathbf{K}|$.

Next, using the Maxwell equation, the continuity equation, and the condition $\mathbf{k}\perp\mathbf{B}$, we obtain the London equation[120]

$$\mathbf{B} + \lambda_\pi^2\,\mathrm{curl}\,\mathrm{curl}\,\mathbf{B} = 0, \quad (4.30)$$

where $\lambda_\pi = (1/e^2f_\pi^2)^{1/2}$ is the magnetic-field penetration depth. We therefore conclude that the Meissner effect occurs in the material of the core of the neutron star for $\mathbf{k}\perp\mathbf{B}$. In this $\mathbf{k}$, $\mathbf{B}$ geometry, the external magnetic field penetrates the core in the form of a laminar structure[121] that constitutes periodically distributed normal plane layers (parallel to the $\mathbf{k}$, $\mathbf{B}$ plane) of width ξ_π with superconducting regions located between them.

To elucidate the origin of the above structure, we must estimate the critical field H_c and the lower critical field H_{c1} for the creation of the line structure,[122] as well as the lower critical field H'_{c1} for the laminar structure. The first two are given by[83]

$$H_c(\theta=\pi/2) = \left[\frac{n^2(g_A^2-1)}{4f_\pi^2} - 2f_\pi^2\right]^{1/2},$$
$$H_{c1}(\theta=\pi/2) = \frac{1}{2}ef_\pi^2\ln(n^3/8ef_\pi^2). \quad (4.31)$$

The lower critical field for the appearance of the laminar structure is given by[120]

$$H'_{c1}(\theta=\pi/2)=\frac{H_c(\theta=\pi/2)}{(\delta(\theta=\pi/2))^{1/2}}=\left[\frac{2ef_\pi^5}{n}\cdot\left(g_A^2-1-\frac{8f_\pi^4}{n^2}\right)\right]^{1/2}\qquad(4.32)$$

where $\delta=n^3/8ef_\pi^7$ is the Ginzburg–Landau parameter of the pion condensate in the case of the limiting condensate field.

It is clear from (4.31) and (4.32) that the fields H_c and H_{c1} increase with increasing n ($n\gg n_{c1}$): H_c rises linearly and H_{c1} logarithmically, whereas H'_{c1} decreases in inverse proportion to $n^{1/2}$. This means that, for high densities, the magnetic field penetrates the core with the structure of the laminar state.

Let us now consider the general case for which $\theta=\theta_0$. Using the continuity condition, the condition $\mathbf{k}\perp\mathbf{B}$, and the fact that much of the pion condensate is in the homogeneous superconducting state with $\theta=\theta_0$ and $\mathbf{A}(r)=0$, we obtain the London equation[120] with λ_π given by

$$\lambda_\pi=\Big(e^2f_\pi^2\sin^2\theta_0\times\Big[1-\frac{\cos^2\theta_0[1+(g_A^2-1)\sin^2\theta_0]}{\{\cos^2\theta_0+\sin^2\theta_0[g_A^4-(g_A^2-1)^2\cos^2\theta_0]\}^{3/2}}\Big]\Big)^{-1/2}.\qquad(4.33)$$

For a developed condensate, the second term in brackets vanishes and λ_π is given by the above expression. When $\theta_0\to 0$, we have $\lambda_\pi\to\infty$, i.e., the medium undergoes a transition to the normal state.

The equilibrium angle θ_0 and the critical density n_{c1} for the appearance of the condensate are given by the following relations:[83]

$$\left(\frac{n}{n_{c1}}\right)^2\cos\theta_0=[1+(g_A^2-1)\sin^2\theta_0]^2,\qquad n_{c1}=\frac{2f_\pi^2}{g_A(g_A^2-1)^{1/2}}.\qquad(4.34)$$

The general expressions for H_c, H_{c1}, and H'_{c1} are given in Ref. 20. Although these expressions also vary in the present case, the dependence on the nucleon density for high densities n is the same as for a developed condensate.

We therefore conclude that, in the σ-model, the pion condensate is a type II superconductor in which the mixed-state laminar structure is always realized. We note that the result reported in Ref. 84 and the above discussion are in conflict with Ref. 83 in which there is an error in the estimated structure of the condensate.

5. GLITCHES IN THE ROTATIONAL PERIOD OF A PULSAR

As the volume of observational data has continued to grow, it has became clear that large period glitches, followed by slow relaxation, are a common feature of pulsars and, despite the difference in their size, the glitches have a common origin. A qualitatively correct description of the glitches can be achieved already within the framework of the simple two-component model of a pulsar.[123] The basic point is that a pulsar consists of weakly-coupled normal and superconducting components.[69] As it evolves, the neutron star loses energy and angular momentum, so that its angular velocity Ω gradually decreases. If one of the components of the star does not for some particular reason succeed in rearranging itself in accordance with the equilibrium state of the system (which depends on Ω), an unstable state arises in the system. The moment of inertia I_c of the normal component of the neutron star can then undergo an abrupt change with a consequent abrupt change $(\Delta\Omega)_0$ in the angular velocity:

$$\frac{\Delta I_c}{I_c}=-\frac{(\Delta\Omega)_0}{\Omega_0}.\qquad(5.1)$$

The second component, i.e., the neutron superfluid, does not initially undergo this change and retains its angular velocity. The superfluid and normal components then begin to interact through frictional forces and, gradually, after an interval of time τ, begin to rotate synchronously. Some friction is also found to arise between electrons and normal neutrons within the normal cores of vortices. The angular velocity of a pulsar after a glitch is well described by the so-called glitch function[28]

$$\Omega(t)=\Omega_0(t)+(\Delta\Omega)_0(Qe^{-t/\tau}+1-Q),\qquad(5.2)$$

where $\Omega_0(t)$ is the value of Ω at time t, obtained by extrapolation on the assumption that $(\Delta\Omega)_0=0$ and the parameters Q and τ are deduced from a comparison with observations. The final change in the angular velocity is $(1-Q)(\Delta\Omega)_0$ and is related to the total moment of inertia I as follows:

$$\frac{\Delta I_c}{I}=-\frac{(\Delta\Omega)_0}{\Omega_0}\cdot(1-Q).\qquad(5.3)$$

It follows from (5.1) and (5.2) that Q is the ratio of the moment of inertia of the superfluid component to the total moment of inertia.

Whereas the above explanation of the behavior of a pulsar after a glitch is generally accepted, several hypotheses have been put forward to explain the onset of instability that leads to a glitch, and for the mechanisms responsible for the transfer of angular momentum to the normal component. These hypotheses include explanations based on magnetospheric instabilities,[124,125] instabilities in the motion of vortices,[126] sudden releases of particles held in regions with closed lines of force,[127] and abrupt increases in the internal temperature of the star.[128] They all encounter specific difficulties, but are capable of explaining some of the known facts. The theory of starquakes[129] was initially rather attractive, and its essence may be summarized as follows. The equilibrium shape of a neutron star corresponds to a particular flattening at the poles due to its rotation. As Ω decreases, the equilibrium shape of the star changes, i.e., there is a reduction in its eccentricity. Since the solid envelope cannot uniformly follow the change in the equilibrium configuration, an instability sets in. When the mismatch between the shape of the neutron star and its equilibrium configuration reaches the critical value, the shell cracks and the abrupt reduction in the moment of inertia of the star produces a step change in its angular velocity. Unfortunately, this theory can explain neither the large size of such steps nor the interval between them for the Vela pulsar PSR 0833-45.

Another approach to the interpretation of pulsar glitches involves the dynamics of vortex lines in superfluid stellar regions. The essential point here is that a particular fraction of the superfluid may not be in the state of equilibrium and may rotate differentially relative to the remainder of the star. This is due to the pinning of neutron vortices to nuclei in the inner crust (Aen-phase) of the neutron star.[130] The neutron superfluid in the core (npe-phase) of the star is assumed to be rigidly coupled to the crust, and the only free component of the star is the neutron superfluid in the Aen-phase. It contains only a few per cent of the stellar moment of inertia and is responsible for the long characteristic relaxation time. Since electrons in the npe-phase are rigidly coupled to the crust, this necessarily implies that there is a similar coupling between electrons and the neutron superfluid in the core of the star. This is examined in the next Section.

5.1. Relaxation of electrons on vortex lines in the npe-phase

The coupling of electrons to the neutron superfluid in the npe-phase is due to the scattering of normal electrons by the normal cores of neutron vortex lines. The characteristic time for this scattering can be expressed in terms of the parameters of the superfluid neutrons as follows:[71]

$$\tau_c = \frac{2{,}94 \cdot 10^5 x^{2/3} p \Delta_2}{k_{2F} T_8} \exp\left(\frac{4{,}41\Delta_2^2}{k_{2F}^2 T_8}\right), \qquad (5.4)$$

where x is the ratio of the electron to neutron densities, Δ_2 is the energy gap in MeV, k_{2F} is the neutron wave number measured in fm^{-1}, p is the rotational period in seconds, and T_8 is the reduced temperature, given by $T_8 = 10^{-8}$ T. The strong dependence of τ_c on temperature and the energy gap is due to the fact that the probability of a neutron excitation that scatters the electrons is proportional to $\exp(-\Delta_2/E_{2F}k_B T)$. The magnitude of τ_c ranges from a few years at $T_8 = 0.1$ to a few hours at $T_8 = 1$ for density $\rho_0' = 4.5\times 10^{14}$ g/cm^3.

The authors of Ref. 131 have investigated the relaxation of normal electrons in the stellar core on neutron vortex lines produced by $^3P_2$ pairing of neutrons. Analysis of vortex solutions[132,133] of the Ginzburg–Landau equations has shown that, in the $^3P_2$-state, the neutron vortex lines have a constant magnetization $M_0 = -1.2\times 10^{11}$ G (Ref. 131). The characteristic time for this scattering is

$$\tau_g = \frac{1{,}26 \cdot 10^8 k_{2F} x^{2/3} p}{\Delta_2}. \qquad (5.5)$$

The scattering time for electrons by neutron vortices with a spontaneous magnetic moment depends on Δ_2 and T, i.e., $\tau_g \sim \Delta_2^{-1}(T)$. The magnitude of τ_g for $\rho_0' = 4.5\times 1014$ g/cm^3 is of the order of one year.

The scattering time τ_v for electrons on the magnetic field of neutron vortices was calculated in Ref. 134. Such fields arise as a result of the drag effect.[97] The field of an individual vortex is given by

$$\mathbf{B} + \lambda^2 \text{curl curl } \mathbf{B} = \frac{\Phi_1}{\pi\xi_2^2}\cdot \mathbf{i}_2\theta(\xi_2 - \rho), \qquad (5.6)$$

where $\theta(\xi_2 - \rho)$ is the Heaviside function. This equation allows for the fact that the normal core of a neutron vortex that contributes significantly to scattering has a finite radius ξ_2. The scattering time is given by[134]

$$\tau_v^{-1} = 11{,}5p^{-1}\left(\frac{m_1^* - m_1}{m_1}\right)^2 \frac{\beta}{\alpha}\cdot(1 - g(\beta)), \qquad (5.7)$$

where the expression for the coefficient $g(\beta)$ is given in Ref. 134 and the remaining coefficients are given by

$$\alpha = 3{,}85x^{1/3}\rho_{14}^{2/3}\frac{m_2}{m_2^*}\Delta_2^{-1}, \quad \beta = 0{,}54x^{1/2}\rho_{14}^{5/6}\left(\frac{m_1}{m_1^*}\right)^{1/2}\frac{m_2}{m_2^*}\Delta_2^{-1}; \qquad (5.8)$$

where $\rho_{14} = 10^{-14}\rho$. The magnitude of τ_v for a given density ρ_0' is of the order of one second. However, a dense bundle of proton lines appears around each neutron line[116] and, as will be seen below, the bundle is coupled to the neutron lines by the electromagnetic interaction. We therefore have to calculate the electron scattering time τ_{eff} on these proton vortices.

Since the core of a proton vortex line has a finite radius, the scattering time is given by[135]

$$\tau_{eff}^{-1} = \frac{(\pi/3)}{32}\cdot k_e c\left(\frac{e^2 k_e}{m_1 c^2}\right)^{3/2} \frac{k}{(1+k)^{3/2}}\left(\frac{\xi_1}{\lambda}\right)^{2/3|k|} \qquad (5.9)$$

where k_e is the electron wave vector and k is the drag coefficient. Our calculations show that the scattering time τ_{eff} is much shorter than all other times, and depends significantly on the density of the npe-phase, decreasing with increasing density. For example, for $\rho = 2\times 10^{14}$ g/cm^3, the characteristic time is $\tau_{eff} = 10^{-14}$ s whereas for $\rho_0' = 4.5\times 10^{14}$ g/cm^3, we have $\tau_{eff} = 10^{-15}$ s. These results suggest that there is very strong coupling between electrons and proton vortices. The latter are coupled to neutron vortices by the electromagnetic interaction.

Maxwell's equations can be shown to lead to the following equation for the magnetic-field perturbation $\delta\mathbf{B}$ due to the glitch $(\Delta\vec{\Omega})_0$ in the angular velocity at time $t = 0$:

$$\frac{1}{c^2}\frac{\partial^2\delta\mathbf{B}}{\partial t^2} - \Delta\delta\mathbf{B} + \frac{1}{\lambda^2}\delta\mathbf{B} = -\frac{8\pi\rho_1 e}{m_1 c}\theta(t)(\Delta\vec{\Omega})_0. \qquad (5.10)$$

It is clear from this expression that the the magnetic-field perturbation propagates with the velocity of light. Since proton vortices are coupled to neutron vortices by the magnetic field, the relaxation time of the velocity of a neutron vortex relative to the ambient proton vortices is of the order of $r_1/c \sim 10^{-14}$ s, i.e., it is comparable with the relaxation time of the electron velocity relative to proton vortices. Consequently, the entire npe-phase may be regarded as undergoing rigid-body rotation, since the longest relaxation time is of the order $R_1/c \sim 10^{-4}$ s. Normal electrons, on the other hand, couple the crust to the npe-phase with characteristic times of the order of 1 s (Ref. 136).

We therefore conclude that the reason for the long relaxation times of the angular velocity of pulsars after a glitch must be sought outside the core of the neutron star.

5.2. Dynamics of neutron vortices and pulsar glitches

As already noted, the most promising models capable of explaining the large glitches in pulsar periods and their subsequent slow relaxation are based on neutron vortex dynamics. The slow relaxation is entirely due to a small part of the superfluid, namely, the neutron superfluid in the Aen-phase of the neutron star.

The equations describing vortex lattice dynamics, and the response of the lattice to a sudden change in the angular velocity of the container, were obtained in Ref. 137. Without going into details of the interaction between normal and superfluid components, it was shown that the initial step in the angular velocity of the normal part of the system was followed by an exponential smoothing out of the initial disturbance.

Consider the equilibrium situation in which the star rotates with angular velocity Ω_c. The angular velocity Ω_s of the superfluid is determined by the distribution of vortices with constant density N_2, given by (2.3).

A change in the angular velocity Ω_c of the star is accompanied by the radial motion of vortices relative to the normal component. This motion occurs so that the superfluid component reaches the state in which it rotates synchronously with the normal component, which is achieved by an increase (if $\dot{\Omega}_c > 0$) or a reduction ($\dot{\Omega}_c < 0$) in the vortex density. In the former case, the vortices move radially toward the axis of rotation, whereas in the latter case they move toward the stellar surface. The rate of change of the angular velocity Ω_s is related to the velocity v_r of the vortices as follows:[138]

$$\dot{\Omega}_s = -\frac{\varkappa_2 N_2 v_r}{r} = -\left(2\Omega(r) + r\frac{\partial\Omega(r)}{\partial r}\right)\frac{v_r}{r}, \tag{5.11}$$

where r is the distance from the axis of rotation of the star and we assume that the number of vortices is conserved, i.e., $\partial N_2/\partial t + \mathrm{div}(N_2 v_r) = 0$. The secular increase in the period of the pulsar is thus seen to be accompanied by the radial motion of vortices toward the surface of the neutron star. This motion will thus slow down the rotation of the superfluid component in accordance with the reduction in the angular velocity of the crust. However, the pinning of the neutron vortices to nuclei is possible in the Aen-phase and may prevent the slowing down of the superfluid component in this phase which will rotate more rapidly than the normal component. A velocity difference is thus established between superfluid and normal components, which leads to an instability in the system. In particular, the energy and the angular momentum of the differentially rotating superfluid component are the sources of glitches in pulsar periods. The pinning of neutron vortices to nuclei in the Aen-phase depends on the parameters of the nuclei and the energy gap of the neutron superfluid, inside and outside the nuclei. Since the energy gap depends on the density of the material, and lies in the range 0.1–1 MeV in the Aen-phase, the pinning energy is also different for different parts of the star: in some regions the vortex lines are rigidly pinned to the crust, whereas elsewhere the pinning is much weaker or may be absent altogether. The pinning of neutron vortices to the nuclei is energetically favorable if this produces a reduction in the energy necessary to establish their normal cores. In the opposite case, it is energetically more favorable for the vortices to be located between the nuclei. Since the condensation energy density is given by $\varepsilon_K = -(3/8)\Delta_2^2 n_2 E_{2F}^{-1}$, where n_2 is the neutron density and E_{2F} is the Fermi energy, we can write the pinning energy density per nucleus in the form[139]

$$E_p = \frac{3}{8}[(\Delta_2^2 n_2 E_{2F}^{-1})_{out} - (\Delta_2^2 n_2 E_{2F}^{-1})_{in}]V; \tag{5.12}$$

where the subscripts 'out' and 'in' represent the local values of Δ_2, n_2, and E_{2F} of superfluid neutrons outside and inside nuclei, respectively, V is the volume occupied by the core of a vortex, and R_N is the nuclear radius. Despite the uncertainty in the magnitude of the energy gap as a function of density (the gap is an exponential function of the unknown nucleon-nucleon interaction), these calculations show that pinning is possible for densities in the range $10^{13} - 2\times10^{14}$ g/cm^3 (Ref. 140).

A detailed study of the interaction between vortices and nuclei in the Aen-phase, based on the Ginzburg–Landau theory, was performed in Ref. 141. The superfluid properties of nuclei were obtained by minimizing the free-energy functional, and it was shown that the interaction between vortices and nuclei led to pinning for densities in excess of 10^{13} g/cm^3.

By analogy with the behavior of type II superconductors in the resistive state with small potential differences, F. Anderson and N. *Itoh*[130] *proposed the possibility of thermal* creep in the vortex structure. They assumed that quantum tunneling of thermally activated neutron vortices across pinning barriers was possible in the equilibrium state (in the absence of a glitch), whereby vortices hopped randomly between pinning centers. The radial velocity of the vortex structure is then given by

$$v_r = v_0 \exp\left[-\frac{E_p(\omega_{cr}-\omega)}{k_B T\omega_{cr}}\right], \tag{5.13}$$

where v_0 is the velocity of the vortices in the absence of pinning ($v_0 \sim 10^{-7}$ cm/s), T is the temperature of the crust, $\omega = \Omega_s - \Omega_c$ is the relative angular velocity of the superfluid in normal crust and $\omega_{cr} = (\Omega_s - \Omega_c)_{max}$ is the maximum relative velocity that can be supported by pinning forces. The equation of motion of the vortices, given by (5.11), thus assumes the form

$$\dot{\Omega}_s = -2\Omega_s\frac{v_0}{r}\exp\left[-\frac{E_p}{k_B T}\cdot\frac{\omega_{cr}-\omega}{\omega_{cr}}\right]. \tag{5.14}$$

We note that the characteristic relaxation time for thermal creep is proportional to temperature and is given by

$$\tau_i = \left(\frac{\omega_{cr}}{E_p}\right)_i \frac{k_B T}{|\dot{\Omega}_\infty|} = \frac{\alpha_i T}{|\dot{\Omega}_\infty|}, \tag{5.15}$$

where $\dot{\Omega}_\infty$ is the equilibrium value of $\dot{\Omega}_c$, k_B is the Boltzmann constant, and the subscript i labels the particular pinning layer.

Glitches were interepreted by Anderson and Itoh as being due to the catastrophic detachment of a large number of vortices, when the differential angular velocity reaches a certain critical value. These vortices transfer angular momentum to the crust of the neutron star and thus accelerate its rotation period.[130] The alternative explanation assumes that the resultant stresses in regions with a large energy gap of the neutron condensate are more likely to give rise to the cracking of the crust than the detachment of vortex lines, and thus shift the vortices without detachment.[142] The moment of internal forces transferred to the crust by the superfluid when the angular rotation undergoes a step change $(\Delta\Omega_c)_0$

is given by

$$N(t)=\sum \frac{I_i\dot{\Omega}_\infty}{[1+(e^{t_{0i}/\tau_i}-e^{-t/\tau_i})]}, \tag{5.16}$$

where I_i is the moment of inertia of the Ith pinning region and t_{0i} is the characteristic glitch relaxation time. For regions in which there is no vortex motion, the characteristic glitch relaxation time is[138]

$$t_{0i}=\frac{(\Delta\Omega_c)_0}{|\dot{\Omega}_\infty|}. \tag{5.17}$$

On the other hand, in regions in which vortices are brought into motion as a result of a glitch, this time is given by

$$t_{0i}=\frac{\delta\Omega_i}{|\dot{\Omega}_\infty|}=\frac{X_i\varkappa_2}{2\pi r^2|\dot{\Omega}_\infty|}, \tag{5.18}$$

where $\delta\Omega_i$ is the change in the angular velocity due to a glitch and X_i is the number of moving vortices.

The post-glitch derivative of the angular velocity of a pulsar is given by

$$\dot{\Omega}_c(t)=\frac{I}{I_c}\cdot\dot{\Omega}_\infty-\frac{N(t)}{I_c}. \tag{5.19}$$

Consequently, in this model, the change in the angular velocity is an exponential function of the initial glitch $(\Delta\Omega_c)_0$. In the two-component model, the corresponding dependence is linear. If the characteristic time is $T_{0i}\gg\tau_i$, the time dependence in (5.19) is similar to the Fermi distribution function of statistical physics.

We therefore conclude that the differences between the creep model[138] and the simple two-component model[123] are as follows:

(a) the period glitches and the long relaxation times are due to the pinned superfluid in the crust, which accounts for only a few per cent of the neutron superfluid. This is determined by the observationally confirmed fact that $(\Delta\dot{\Omega}_c/\dot{\Omega}_c)_0\sim I_p/I\sim 10^{-2}$–$10^{-3}$ for 14 glitches in seven pulsars (I_p is the moment of inertia of the pinned superfluid)

(b) this model is essentially nonlinear and describes the response of the superfluid; vortex creep due to an angular velocity glitch is an exponential function of the glitch (in regions in which the vortices do not move) and of the change in the superfluid velocity (in regions in which vortices continue to move during the glitch)

(c) the relaxation times are proportional to the internal temperature of the neutron star, so that the observational data can be used to determine this temperature in pulsars.

5.3. Comparison between the creep model and observational data

The relaxation of the angular velocity of the Vela pulsar PSR 0833-45 after the four glitches of 1969–1979 (Ref. 26) can be explained in terms of vortex creep.[143] The observational data[26] are satisfactorily described by the following equation of motion of the "normal" component:

$$I_c\dot{\Omega}_c(t)=N_{ext}(t)-N_1-N_2-N_A, \tag{5.20}$$

where $N_{ext}=I\dot{\Omega}_\infty$ is the moment of external forces acting on the pulsar, and N_1 and N_2 are the moments of internal forces given by (5.16) and (5.17) with the corresponding relaxation times τ_1 and τ_2. These internal moments constitute the average response of two different pinning layers in which the vortices are stationary. The third region associated with the motion of vortices is represented by the moment N_A which, in the first approximation, is given by

$$N_A\approx\dot{\Omega}_\infty\frac{I_At}{t_{0B}}, \tag{5.21}$$

where I_A is the moment of inertia of the superfluid in pinning layers (whenever the vortices become detached and are pinned down again) and t_{0B} is the delay time due to setting X_i in (5.18) equal to the total number of detaching vortices.

Good agreement with observational data can be obtained by taking $\tau_1=3$ days and $\tau_2=60$ days for each of the four glitches of pulsar PSR 0833-45 in 1969–1979. The analysis performed in Refs. 143 shows that these two pinning regions correspond, respectively, to superweak and weak pinning, characterized by $\langle\alpha_{SW}\rangle 2\times10^{-17}\text{d}\cdot\text{K}^{-1}\text{s}^{-2}$ and $\langle\alpha_w\rangle\sim4\times10^{-16}\text{d}\cdot\text{K}^{-2}\text{s}^{-2}$. The internal temperature of pulsar PSR 0833-45, determined from the observed relaxation times, is 1.5×10^7 K. The observed relaxation of the angular velocity of the Crab pulsar PSR 0531 + 21 can be explained by taking the relaxation times to be $\tau_1=3$ days and $\tau_2=60$ days. The former corresponds to the motion of vortices across the superweak pinning region and the second across the weak pinning region.[144] A constant relative change in the derivative of the angular velocity, namely, $\Delta\dot{\Omega}_c/\dot{\Omega}_c=2\times10^{-4}$, which persisted for 1500 days,[145] was observed after 1975. This constant relative variation is explained in the nonlinear creep model by the appearance of a constant internal moment of force in regions with a vortex excess. The relaxation time of this constant moment is $\tau'>1500$ days.[144]

The internal temperature of pulsar PSR 0531 + 21, deduced from an analysis of the relaxation times τ_1 and τ_2, is 3.8×10^8 K. The surface temperatures of pulsars PSR 0833-45 and PSR 0531 + 21 are found to be $T_{\infty1}=3\times10^5$ and $T_{\infty2}=1.6\times10^6$ K. These temperatures are lower than the upper bounds deduced for these pulsars from observations recorded by the Einstein x-ray observatory.[146]

For old pulsars that have already expended most of their initial thermal-energy reserves, the main source of energy may be internal dissipation by vortex creep. The surface temperature T_S can be obtained[144] by equating the energy dissipated per unit time to the thermal luminosity of the stellar surface. If all the old pulsars have the same pinning layers as PSR 0833-45 and PSR 0531 + 21, their temperature is determined by energy dissipation, and the relaxation times for superweak and weak pinning depend on the rate of change of angular velocity as follows:[144]

$$\tau_{SW}=220\left(\frac{I_{p,43}\bar{\omega}_{cr}}{R_6^2}\right)^{1/4}|\dot{\Omega}_{-14}|^{-3/4}\text{days}, \tag{5.22}$$

$$\tau_W=4{,}4\cdot10^3\left(\frac{I_{p,43}\bar{\omega}_{cr}}{R_6^2}\right)^{1/4}|\dot{\Omega}_{-14}|^{-3/4}\text{ days}, \tag{5.23}$$

where $\bar{\omega}_{cr}$ is the average of ω_{cr} evaluated over all the pinning layers. The observational data for PSR 1929 + 10 can be analyzed to show that $I_{p,43}\overline{\omega}_{cr} \leqslant 1$.

The observed relaxation of the angular velocity of the old pulsar PSR 0525 + 21 can be explained by taking $\tau_1 = 150$ days and $\tau_2 = 3000$ days (Ref. 144). The "fast" relaxation time calculated from (5.22) is $\tau_{SW} \approx 140$ days, which is in good agreement with the observed value of τ_1. We note that the value of τ_1 is in agreement with the assumption that the main source of energy of this pulsar is dissipation due to vortex creep.

After the large glitch of pulsar PSR 0355 + 54 in 1985 ($\Delta\Omega/\Omega = 4.4\times 10^{-6}$), the observed relaxation can be described as follows:[25]

$$\Delta\Omega_c(t) = [(\Delta\Omega_c)_0 - \Delta\Omega_2] + \Delta\dot{\Omega}_1\cdot t + \Delta\Omega_2\cdot\exp(-t/\tau), \quad (5.24)$$

$$\Delta\dot{\Omega}_c(t) = \Delta\dot{\Omega}_1 + \Delta\dot{\Omega}_2\cdot\exp(-t/\tau) = \Delta\dot{\Omega}_1 - \frac{\Delta\Omega_2\exp(-t/\tau)}{\tau}, \quad (5.25)$$

where $\Delta\Omega_c(t)$ and $\Delta\dot{\Omega}_c(t)$ are the changes in these quantities relative to their values prior to the glitch. $\Delta\Omega_2/\Omega_2 = 4.2\times 10^{-9}$, $\Delta\dot{\Omega}_2/\dot{\Omega} = 0.039$. Consequently, one thousandth of the initial step $\Delta\Omega$ relaxes exponentially with relaxation time $\tau = 44$ d. Moreover, there is a constant relative step $\Delta\dot{\Omega}_1$ ($\Delta\dot{\Omega}_1/\dot{\Omega} = 0.0059$) that determines I_p/I in the regions in which vortex creep ceases as a result of the glitch.

In previous applications of creep theory, the superfluid in the pinning region did not participate in the slowing down of rotation during the characteristic times (delay times) given by (5.17) and (5.18). The values of these constants for PSR 0355 + 54 are 4.9 y and 832 y, respectively.[147] Consequently, a constant step $\Delta\dot{\Omega}_1$ will be observed for 4.9 y after the glitch.

The exponential term in (5.24) cannot be explained in this way because it does not contain the delay times. Even a 77-day uncertainty in the precise date of the glitch is too small to mask these much longer times. These particular terms can be explained by a linear regime that is established in the vortex creep model if $\eta = (|\dot{\Omega}_\infty| r/4\Omega_0 v_0)\exp(E_p/k_B T) < 1$. The nonlinear regime is established when this condition is not met.

The derivative of the angular velocity is a linear function of the glitch $(\Delta\Omega_c)_0$ and is given by[147]

$$\dot{\Omega}_c(t) = \dot{\Omega}_\infty - \frac{I_2}{I}\cdot\frac{(\Delta\Omega_c)_0}{\tau_l}\cdot\exp[-t(\tau_l I_c/I)^{-1}], \quad (5.26)$$

where I_2 is the moment of inertia of the pinned superfluid in the linear creep region, $I_2 < I_p \ll I_c$, and τ_l is the corresponding relaxation time given by

$$\tau_l = \frac{k_B T}{E_p}\cdot\frac{\omega_{cr} r}{4\Omega_0 v_0}\cdot\exp\left(\frac{E_p}{k_B T}\right). \quad (5.27)$$

The quantity $\Delta\Omega_2 = (\Delta\Omega_c)_0 I_2/I$ can now be obtained from (5.26). Analysis of observational data shows that the moment of inertia is $I_2/I \approx 9.5\times 10^4 - 5.5\times 10^{-3}$. This is in agreement with the result $I_p/I = 0.0059$ obtained for the nonlinear creep regions. It is also in agreement with theoretical calculations of the moment of inertia of a pinned superfluid and with values obtained by analyzing observational data for other pulsars. The analysis reported in Ref. 47 shows that the linear creep region corresponds to superweak pinning with energy $E_p = 0.05$ MeV.

Consequently, the linear regime is established in some pinning layers of pulsar PSR 0355 + 54, whereas the nonlinear regime of vortex creep (the term containing $\Delta\dot{\Omega}_1$) is realized elsewhere.

Pinning and vortex-creep models rely on the presence of a dissipative process that transfers the angular momentum of the superfluid to the solid crust and determines the minimum dynamic coupling time τ_d between this fluid and the crust. Observations of the eighth glitch in pulsar PSR 0833-45 suggest that τ_d should be less than 2 min.[148,149] The value of τ_d due to the scattering of electrons by the electric charge induced around neutron vortices is of the order of a few months or even one year.[150] Still longer τ_d is obtained for the scattering of electrons by the normal cores of neutron vortices in the Aen-phase.[71] Much lower values of τ_d are obtained for the dissipative process discussed in Ref. 151, which arises because of the inhomogeneity of the order parameter in a neutron vortex.[152] For pulsar PSR 0833 − 45, this time is $\tau_d = 3.6\times 10^{-2}$ s (Ref. 151), which is in good agreement with observational data and confirms the model in which pulsar glitches are interpreted in terms of the sudden liberation of a large number of pinned vortex lines in the Aen-phase. Models based on the dynamics of neutron vortices are at present the only ones capable of providing a satisfactory explanation of all the observational data on pulsar glitches.

It is our pleasant duty to thank L. P. Pitaevskiĭ for reading our manuscript and for a number of valuable suggestions.

[1] F. G. Smith, *Pulsars*, Cambridge University, Cambridge, 1977 [Russ. original, Mir, M., 1979].
[2] R. N. Manchester and J. H. Taylor, *Pulsars* Freeman, S. F., 1977 [Russ. transl., Mir, M., 1980].
[3] A. Hewish, S. J. Bell, J. D. H. Pilkington *et al. Nature* 709, 217 (1968).
[4] T. Gold, *ibid.* 218, 731 (1968).
[5] G. S. Saakyan, *Equilibrium Configurations of Degenerate Gaseous Masses* [in Russian], Nauka, M., 1972.
[6] J. Trumper, W. Pletsch, C. Reppin *et al.*, Mitt. Astron. Ges. No. 42, 120 (1977).
[7] J. Trumper, W. Pletsch, C. Reppin *et al.*, Astrophys. J. **219**, 105 (1978).
[8] J. Daugherty and J. Ventura, Astron. and Astrophys. **61**, 723 (1977).
[9] P. Meszaros, *ibid.*, **63**, 19 (1978).
[10] M. Goe, A. Engel, and Quenby *et al.*, *Nature* **268**, 508 (1977).
[11] W. A. Wheaton and C. Howie *et al.*, Bull. Am. Astron. Soc. **10**, 506 (1978).
[12] P. C. Joss and S. A. Rappaport, Ann. Rev. Astron. and Astrophys. **22**, 537 (1984).
[13] J. C. Long, W. A. Mahoney, J. B. Willet, and W. N. Johnson, Astrophys. J. **231**, 896 (1979).
[14] M. S. Strickman, J. D. Kurfess, and W. N. Johnson, Astrophys. J. Lett. **253**, 23 (1982).
[15] V. V. Vitkevich (ed.), *Pulsars* [collection of transl. into Russian], Mir, M., 1971.
[16] F. Pacini, Nature **216**, 567 (1967).
[17] J. E. Gunn and J. P. Ostriker, *ibid.* **221**, 454 (1969).
[18] J. P. Ostriker and J. E. Gunn, Astrophys. J. **157**, 1395 (1969).
[19] D. W. Richards and J. Comella, Nature **222**, 551 (1969).
[20] M. C. Weisskopf, R. F. Elsner, and W. Darbro *et al.*, Astrophys. J. **267**, 711 (1983).
[21] D. C. Backer, S. R. Kulkarni, C. Heiles *et al.*, *Nature* **300**, 615 (1982).
[22] M. M. Davis, J. H. Taylor, J. M. Weisberg, *et al.*, *ibid.* **315**, 547 (1985).
[23] Y. Terzian and T. E. Nordgren, Preprint, Cornell University, 1990.
[24] T. V. Shabanova, *Physics of Neutron Stars: Pulsars and Bursters* [in Russian], Leningrad, 1988, p. 168.
[25] A. G. Lyne, Nature **326**, 569 (1987).
[26] G. S. Downs, Astrophys. J. **249**, 687 (1981).
[27] P. M. McCulloch, P. A. Hamilton, G. W. R. Royle, and R. N. Manchester, *Nature* **302**, 319 (1983).

[28] D. Pines, Pulsars and Compact X-ray Sources: Cosmic Laboratories for the Study of Neutron Stars and Hadron Matter, Review paper presented to Int. Coll. on Dense Matter Physics, Paris, 1977.
[29] R. N. Manchester, L. N. Newton, P. A. Hamilton, and W. M. Goss, Mon. Nat. RAS. **202**, 269 (1983).
[30] L. M. Newton, R. N. Manchester, and J. D. Cooke, *ibid.* **194**, 341 (1981).
[31] P. R. Backus, J. H. Taylor, and M. Damashek, Astrophys. J. **255**, L63 (1982).
[32] A. G. Lyne and R. Pritchard, Mon. Not. R. Astron. Soc. **229**, 223 (1987).
[33] G. S. Downs, Astrophys. J. **257**, L67 (1982).
[34] Dzh. S. Tsakadze and S. Dzh. Tsakadze, Zh. Eksp. Teor. Fiz. **64**, 1816 (1973) [Sov. Phys. JETP **37**, 918 (1973)].
[35] Dzh. S. Tsakadze and S. Dzh. Tsakadze, Pis'ma Zh. Eksp. Teor. Fiz. **18**, 605 (1973) [JETP Lett. **18**, 355 (1973)].
[36] Dzh. S. Tsakadze and S. Dzh. Tsakadze, *ibid.* **22**, 301 (1975) [**22**, 139 (1975)].
[37] L. D. Landau, Phys. Zs. Sowjetunion **1**, 285 (1932).
[38] W. Baade and F. Zwicky, Phys. Rev. **46**, 76 (1934).
[39] J. R. Oppenheimer and G. M. Volkoff, Phys. Rev. **55**, 374 (1939).
[40] V. A. Ambartsumyan and G. S. Saakyan, Astron. Zh. **38**, 785 (1961) [Sov. Astron. **5**, 601 (1962)].
[41] V. A. Ambartsumyan and G. S. Saakyan, *ibid.* **1016**, 1961.
[42] G. Sahakian and Yu. Vartanian, Nuovo Cimento **30**, 82 (1963).
[43] G. S. Saakyan and Yu. L. Vartanyan, Astron. Zh. **41**, 193 (1964) [Sov. Astron. **8**, 147 (1964)].
[44] S. L. Shapiro and S. A. Teukolsky, *Black Holes, White Dwarfs, and Neutron Stars*, Wiley-Interscience, 1983 N.Y. [Russ. transl. Mir, M., 1985].
[45] A. B. Migdal, Zh. Eksp. Teor. Fiz. **61**, 2209 (1971) [Sov. Phys. JETP **34**, 1184 (1972)].
[46] R. Sawyer and D. Scalapino, Phys. Rev. D **7**, 953 (1973).
[47] J. Bahcall and R. A. Wolf, Phys. Rev. Lett. **14**, 343 (1965).
[48] J. Bahcall and R. A. Wolf, Phys. Rev. **140**, 1452 (1965).
[49] S. Tsuruta, Phys. Rep. **56**, 237 (1979).
[50] A. B. Migdal, A. J. Chernoutsan, and I. N. Mishustin, Phys. Lett. **83**, 158 (1979).
[51] Yu. F. Berezin, O. E. Dmitrieva, and N. N. Yanenko, Pis'ma Astron. Zh. **8**, 86 (1982) [Sov. Astron. Lett. **8**, 43 (1982)].
[52] Yu. L. Vartanyan and G. B. Alaverdyan, Astrofizika **31**, 111 (1989). [Astrophysics **31**, 482 (1989)].
[53] D. Campbell, R. Dashen, and J. Manassah, Phys. Rev. **D12**, 979 (1975).
[54] A. B. Migdal, *Fermions and Bosons in Strong Fields* [in Russian], Nauka, M., 1978.
[55] R. C. Malone, M. B. Johnson, and H. A. Bethe, Astrophys. J. **199**, 741 (1975).
[56] W. D. Arnett and R. L. Bowers, Astrophys. J., Suppl. S. **33**, 415 (1977).
[57] J. Bardeen, L. N. Cooper, and J. R. Schreiffer, Phys. Rev. **108**, 1175 (1957).
[58] N. N. Bogolyubov, Dokl. Akad. Nauk SSSR **52**, 119, 1958 [Sov. Phys. Dokl. **3**, 279 (1958)].
[59] A. Bohr, B. Mottelson, and D. Pines, Phys. Rev. **110**, 936 (1958).
[60] S. T. Belyaev, Mat. Fys. Dan. Vid. Selsk **31**, 3 (1959).
[61] V. G. Solov'ev, Zh. Eksp. Teor. Fiz. **35**, 823 (1958) [**8**, 572 (1959)].
[62] A. B. Migdal, Zh. Eksp. Teor. Fiz. **37**, 249 (1959) [Sov. Phys. JETP **10**, 176 (1960)].
[63] V. L. Ginzburg and D. A. Kirzhnitz, Zh. Eksp. Teor. Fiz. **47**, 2006 (1964) [Sov. Phys. JETP **20**, 1346 (1965)].
[64] R. A. Wolf, Astrophys. J. **145**, 166 (1966).
[65] L. P. Pitaevskii, Zh. Eksp. Teor. Fiz. **37**, 1794 (1959) [Sov. Phys. JETP **10**, 1267 (1960).
[66] P. W. Anderson and P. Morel, Phys. Rev. **123**, 1911 (1961).
[67] M. Hoffberg, A. E. Glassgold, R. W. Richardson, and M. Ruderman, Phys. Rev. Lett. **24**, 775 (1970).
[68] T. Takasuka, Prog. Theor. Phys. **48**, 1517 (1972).
[69] G. Baym, C. Pethick, and D. Pines, *Nature* **224**, 673 (1969).
[70] Yu. M. Bruk, Astrofizika **9**, 237 (1973). [Astrophysics **9**, 134 (1973)].
[71] F. C. Feibelman, Phys. Rev. D **4**, 1589 (1971).
[72] L. Amundsen and E. Ostgaard, Nucl. Phys. A **437**, 487.
[73] L. Amundsen and E. Ostgaard, *ibid.* **442**, 163.
[74] N. C. Chao, J. Clark, and C. H. Tang, Nucl. Phys. A. **179**, 320 (1972).
[75] R. V. Reld, Ann. of Phys. **50**, 411 (1968).
[76] R. Tamagaki, Prog. Theor. Phys. **39**, 91 (1968).
[77] C. H. Yang and J. Clark, Nucl. Phys. A **174**, 49 (1971).
[78] T. Takatsuka, Prog. Theor. Phys. **71**, 1432 (1984).
[79] J. M. C. Chen, J. Ckark, E. Krotscheck, and R. A. Smith, Nucl. Phys. A **451**, 509 (1986).
[80] S. Tsuruta and A. Cameron, Can. J. Phys. **44**, 1863 (1966).
[81] G. S. Adzhyan and Yu. L. Vartanyan, Astrofizika **7**, 237 (1971). [Astrophysics **7**, 136 (1971)].
[82] M. B. Richardson, H. M. van Horn *et al.*, Astrophys. J. **255**, 624 (1982).
[83] B. J. Harrington and H. K. Shepard, Phys. Rev. D **19**, 1713 (1979).
[84] D. N. Voskresenskii and N. Yu. Anisimov, Zh. Eksp. Teor. Fiz. **78**, 28 (1980) [Sov. Phys. JETP **51**, 13 (1980)].
[85] E. I. Andronikashvili, Yu. G. Mamaladze, S. G. Matinyan, and Dzh. S. Tsakadze, Usp. Fiz. Nauk **73**, 3 (1961) [Sov. Phys. Usp. **4**, 1 (1961)].
[86] R. E. Packard, Phys. Rev. Lett. **28**, 1080 (1972).
[87] Dzh. S. Tsakadze and S. Dzh. Tsakadze, Usp. Fiz. Nauk **115**, 503 (1975) [Sov. Phys. Usp. **18**, 242 (1975)].
[88] D. N. Sedrakyan and G. K. Sivvide, Astrofizika **15**, 359 (1979).
[89] I. M. Khalatnikov, *Theory of Superfluidity* [in Russian], Nauka, M., 1971.
[90] L. V. Kiknadze and Yu. G. Mamaladze, Fiz. Nizk. Temp. **6**, 413 (1980) [Sov. J. Low Temp. Phys. **6**, 195 (1980)].
[91] D. N. Sedrakyan and K. M. Shakhabasyan, Dokl. Akad. Nauk Arm. SSR, **70**, 28, 1980.
[92] I. M. Khalatnikov, Zh. Eksp. Teor. Fiz. **32**, 653 (1967) [Sov. Phys. JETP **5**, 542 (1957)].
[93] I. M. Khalatnikov, Pis'ma Zh. Eksp. Teor. Fiz. **17**, 534 (1973) [JETP Lett. **17**, 386 (1973)].
[94] A. F. Andreev and E. P. Bashkin, Zh. Eksp. Teor. Fiz. **69**, 319 (1975) [Sov. Phys. JETP **42**, 164 (1975)].
[95] D. N. Sedrakyan, K. M. Shakhabasyan, and G. A. Vardanyan, Uch. Zap. EGU, No. 2, 72 (1979).
[96] D. N. Sedrakyan and K. M. Shakhabasyan, *ibid.* No. 1., 46 (1980).
[97] L. P. Gor'kov, Zh. Eksp. Teor. Fiz. **34**, 735 (1958) [Sov. Phys. JETP **7**, 505 (1958)].
[98] A. A. Abrikosov, L. P. Gor'kov, and I. A. Dzyaloshinskiĭ, *Methods of Quantum Field Theory in Statistical Physics*, Prentice Hall, 1963 [Russ. original, Fizmatgiz, M., 1962].
[99] L. P. Gor'kov, Zh. Eksp. Teor. Fiz. **36**, 1918 (1959) [Sov. Phys. JETP **9**, 1364 (1959)].
[100] V. P. Ginzburg and L. D. Landau, Zh. Eksp. Teor. Fiz. **20**, 1064 (1950).
[101] V. L. Ginzburg and L. P. Pitaevskii, Zh. Eksp. Teor. Fiz. **34**, 1240, (1958) [Sov. Phys. JETP **7**, 858 (1958)].
[102] G. A. Vardanyan and D. M. Sedrakyan, Zh. Eksp. Teor. Fiz. **81**, 1731 (1981) [Sov. Phys. JETP **54**, 919 (1981)].
[103] J. Bardeen, G. Baym, and D. Pines, Phys. Rev., **156**, 207 (1967).
[104] D. M. Sedrakyan and K. M. Shakabasyan, Astrofizika **16**, 727 (1980) [Astrophysics **16**, 417 (1980)].
[105] V. L. Ginzburg, Dokl. Akad. Nauk SSSR, **156**, 43 (1964) [Sov. Phys. Dokl. **9**, 329 (1964)].
[106] V. L. Ginzburg and L. M. Ozernoĭ, Zh. Eksp. Teor. Fiz. **47**, 1030 (1964) [Sov. Phys. JETP **20**, 689 (1965)].
[107] L. Woltjer, Astrophys. J. **140**, 1309 (1964).
[108] V. L. Ginzburg, Usp. Fiz. Nauk **103**, 393 (1971) [Sov. Phys. Usp. **14**, 83 (1971)].
[109] S. A. Kaplin and V. N. Tsytovich, *Plasma Astrophysics* [in Russian], Nauka, M., 1972.
[110] S. D. Silverstein, Phys. Rev. Lett. **23**, 139 (1969).
[111] J. Pfarr, Zs. Phys. **251**, 152 (1972).
[112] J. Schmid-Burgk, Astron. and Astrophys. **26**, 335 (1973).
[113] R. D. Blandford, J. H. Applegate, and L. Hernquist, Mon. Not. R. Astron Soc. **204**, 1025 (1983).
[114] V. A. Urpin *et al.*, *ibid.*, **219**, 703 (1986).
[115] D. M. Sedrakyan, Astrofizika **18**, 417 (1982). [Astrophysics **18**, 253 (1982)].
[116] D. M. Sedrakyan, K. M. Shakabasyan, and A. G. Movsisyan, Astrofizika **19**, 303 (1983). [Astrophysics **19**, 175 (1983)].
[117] B. I. Verkin and I. O. Kulik, Zh. Eksp. Teor. Fiz. **61**, 2067 (1971) [Sov. Phys. JETP **34**, 1103 (1972)].
[118] D. M. Sedrakyan, G. S. Mkrtchyan, and K. M. Shakabasyan, Izv. Akad. Nauk Arm. SSR, Ser. Fiz. **11**, 385 (1976).
[119] D. M. Sedrakyan, K. M. Shakabasyan, and A. G. Movsisyan, Astrofizika **21**, 547 (1984). [Astrophysics **21**, 556 (1984)].
[120] D. M. Sedrakyan and K. M. Shakabasyan, Astrofizika **28**, 628 (1988) [Astrophysics **28**, 374 (1988)].
[121] B. B. Goodman, Phys. Rev. Lett. **6**, 597 (1961).
[122] A. A. Abrikosov, Zh. Eksp. Teor. Fiz. **32**, 1442 (1957) [Sov. Phys. JETP **5**, 1174 (1957)].
[123] G. Baym, C. Pethick, D. Pines *et al.*, *Nature* **224**, 872 (1969).
[124] J. Scargle and F. Pacini, *Nature*, Phys. Sci. **232**, 144 (1971).
[125] D. H. Roberts and P. A. Sturrock, Astrophys. J. **173**, L33 (1972).
[126] G. Greenstein, and A. G. W. Cameron, *Nature* **222**, 862 (1969).
[127] M. Ruderman, Ann. Rev. Astron. Astrophys. **10**, 427 (1972).
[128] G. Greenstein, Astrophys. J. **231**, 880 (1979).
[129] M. Ruderman, Nature **223**, 597 (1979).

[130] P. W. Anderson and N. Itoh, *ibid.* **256**, 25 (1975).
[131] J. Sauls, D. Stein, and J. Serene, Phys. Rev. D **25**, 967 (1982).
[132] R. W. Richardson, *ibid.* **5**, 1883 (1972).
[133] P. Muzikar, J. Sauls, and J. Serene, *ibid.* **21**, 1494 (1980).
[134] M. A. Alpar, S. A. Langer, and J. Sauls, Astrophys. J. **282**, 533 (1984).
[135] D. M. Sedrakyan, K. M. Shakabasyan, and A. G. Movsisyan, Astrofizika **22**, 137 (1985). [Astrophysics **22**, 84 (1985)].
[136] I. Easson, Astrophys. J. **228**, 257 (1979).
[137] Yu. K. Krasnov, Zh. Eksp. Teor. Fiz. **73**, 348 (1977) [Sov. Phys. JETP **46**, 181 (1977)].
[138] M. A. Alpar, P. W. Anderson, D. Pines, and J. Shalam, Astrophys. J. **276**, 325 (1984).
[139] P. W. Anderson, M. A. Alpar, D. Pines, and J. Shaham, Phil. Mag. A **45**, 227 (1982).
[140] M. A. Alpar, Astrophys. J. **213**, 527 (1977).
[141] R. I. Epstein and G. Baym, *ibid.* **328**, 680 (1988).
[142] M. Ruderman, *ibid.* **203**, 213 (1976).
[143] M. A. Alpar, P. W. Anderson, D. Pines, and J. Shaham, *ibid.* **278**, 791 (1984).
[144] M. A. Alpar, R. Nandkumar, and D. Pines, *ibid.* **288**, 191 (1985).
[145] M. Demianski and M. Proszynski, Mon. Not. R. Astron Soc. **202**, 437 (1983).
[146] F. R. Jnr. Harnden and F. D. Seward, Astrophys. J. **283**, 279 (1984).
[147] M. A. Alpar, K. S. Cheng, D. Pines, and J. Shaham, Mon. Not. R. Astron Soc. **233**, 25 (1988).
[148] IAU Circ. No. 4695 (1988).
[149] *Ibid.* No. 4708.
[150] L. Bildsten and R. I. Epstein, Astrophys. J. **342**, 951 (1989).
[151] D. M. Sedrakyan and A. D. Sedrakyan, Rostock Univ. Preprint TR-UR 3/91, Rostock, 1991.
[152] M. Tinkham, Phys. Rev. Lett. **13**, 804 (1964).
[153] T. V. Shabanova, Astron. Zh. **67**, 536 (1990) [Sov. Astron. **34**, 269 (1990)].
[154] J. McKenna, *Timing Neutron Stars*, Eds. H. Ogelman and E. P. J. van den Heuvel, Kluwer Acad. Publ., Dodrecht, 1989, p. 3.
[155] R. I. Epstein, Astrophys. J. **333**, 880 (1988).

Translated by S. Chomet